

UNIVERSITY OF MINNESOTA

This is to certify that I have examined this copy of a master's thesis by

Emily Elizabeth Bjonnes

and have found that it is complete and satisfactory in all respects, and that any and all revisions required by the final examining committee have been made.

Name of Faculty Co-Advisor

Name of Faculty Co-Advisor

Signature of Faculty Co-Advisor

Signature of Faculty Co-Advisor

Date

GRADUATE SCHOOL

The Plausibility of Venusian Equilibrium Resurfacing Using Monte Carlo Models

A THESIS
SUBMITTED TO THE FACULTY OF THE GRADUATE SCHOOL
OF THE UNIVERSITY OF MINNESOTA
BY

Emily Elizabeth Bjornes

IN PARTIAL FULFILMENT OF THE REQUIREMENTS
FOR THE DEGREE OF
MASTER OF SCIENCE

Dr. Vicki L. Hansen, Dr. John B. Swenson

January 2009

© Emily Elizabeth Bjonnes 2009

Acknowledgements

I'd like to thank co-advisors, Dr. Vicki Hansen and Dr. John Swenson, for taking a chance on me and guiding me through this process. They were indispensable in helping me shape my project and understand how I fit into the larger problem of scientific research. Dr. Barry James, my third committee member from the statistics department, has literally taught me everything I know about statistical models and this project could not have been completed without him. Dr. Richard Maclin of the computer science department helped immensely to get me going with MatLab. Dr. John Goodge, Dr. Howard Mooers, Dr. Thomas Johnson and his wife Kate, Dr. Christina Gallup, Dr. Penny Morton and Dr. Jim Miller of the University of Minnesota Duluth Geology Department were all helpful in getting me through coursework career planning, and maintaining sanity throughout my degree. The help of Ms. Claudia Rock and Ms. Cathy Dzuik was also indispensable as they helped me navigate the red tape of graduate paperwork and assistantships. Outside the geology department, Ms. Mags David, Dr. Kang James, Dr. Katherine Lenz, and Ms. Angie Nichols provided much-needed advice and perspective on my experiences as a graduate student. I'd like to thank my high-school geology teacher, Mrs. Barabaro-Jo Kruczek, for getting me into the geology in the first place with her uncharacteristic enthusiasm and teaching methods. Dr. Jeremy Delaney, Dr. Martha Withjack, Dr. Roy Schlische, Dr. Roger Hewins, Dr. Ken Miller, Dr. Jim Miller, and Dr. Gail Ashley of the Rutgers University Geology Department all helped give me such a solid base in geology that I was able to tackle such a large-scale problem as planetary evolution. Finally, I'd like to thank Dr. Allan Treiman and the late Dr. John Lindsay of the Lunar and Planetary Institute and Dr. Jim Zimbelman of the Center of Earth and Planetary Studies for giving me the chance to work beside them and learn from the best as an intern.

Dedication

This thesis is dedicated first and foremost to my family, Carol Miller, Neil Bjonnes, and Andrew Bjonnes, for keeping me grounded and helping me remember why I wanted to be a scientist in the first place. My extended family—Nanny and Poppy Bjonnes, Delores and Osborne Miller, and my numerous aunts, uncles, and cousins—were always there for me and helped me relax and unwind whenever I could make a trip to see them, which was never often enough. To all the new friends I made in Duluth, Jenny and Brian Goldner, Melissa Berke, Josh Aerie, Bhairavi Shankar, Andrea Johnson, Valerie Gamble, Matt Kuchta, Mandy Little, and Isla Castaneda helped me everyday to not take myself too seriously and tackle problems one day at a time. Natalie Klueg, Amanda Guttman, Darren Neve, Bacon, and the other youngins, you were my life outside the geology department and my head would have definitely exploded without the nights of Guitar Hero, bad horror movies, and deciding at 11 p.m. that this feels like a good night to go dancing. To Erin Murphy, Amy Boyajian, Mary McLaughlin, Daniel Fidalgo Tome, Stephanie Cruz and Allison Seavers—I will always be a Jersey girl at heart and it is all your fault! I miss you guys so much, and even though I moved far away you were never far from my thoughts. Finally, I'd like to thank Heather Dalton for giving me some much-needed understanding and keeping me motivated enough to finish up even when it felt like an impossible task.

Abstract

NASA's Magellan mission took synthetic aperture radar (SAR) images of Venus' surface that showed approximately 975 pristine impact craters distributed near-randomly across the surface. Subsequently proposed resurfacing mechanisms operating on Venus must account for these two first-order, geologic constraints. Two main categories of resurfacing hypotheses have emerged: catastrophic resurfacing and equilibrium resurfacing. Catastrophic resurfacing proposes that the overwhelming majority of the planet was resurfaced instantaneously, and equilibrium resurfacing proposes that smaller areas of Venus' surface were resurfaced throughout time. A previous study using Monte Carlo modeling showed that equilibrium resurfacing in areas of 50, 25, 20, and 10% of the total surface area results in a non-random surficial distribution of impact craters, whereas equilibrium resurfacing in amounts of 0.03 and 0.003% result in too many modified impact craters. Therefore, none of these scenarios meet the geologic constraints. This study focuses on expanding the previous work to include areas of 5, 1, 0.7, and 0.1% of Venus's total surface area, as well as varying the length of resurfacing time to determine this effect on resulting impact crater distributions. I took the average size of an impact crater to be 30 km in diameter and counted the edge effects arising when an impact crater falls between 30 km inward of the resurfacing edge and 30 km outward of the resurfacing edge. Spatial analysis of resulting impact crater distributions consisted of two tests: 1) the distribution of intercrater angles and quantifying the best-fit line when compared to the theoretical relationship, following the method of Turcotte et al (1999), and 2) comparison of resultant vector lengths between a set of 1000 purely random impact crater distributions, 1000 simulated impact crater distributions in each experiment, and the resultant vector of Venus. I find that several scenarios of resurfacing meet the two constraints of Venus' impact crater record, thus providing the much-needed impetus to continue research on equilibrium resurfacing. The number of possible resurfacing histories within each experiment grows as the duration of resurfacing decreases. These results will provide new insight into possible resurfacing mechanisms in Venus' past, showing that catastrophic resurfacing need not be the only interpretation.

Table of Contents

Introduction.....	1
Background.....	6
Methods.....	18
Results.....	26
Discussion.....	29
Conclusion.....	33
Appendix I.....	60
Appendix II.....	62
Appendix III.....	75
References.....	77

List of Tables

Summary of Results.....35

List of Figures

Figure 1.....	36
Figure 2.....	37
Figure 3.....	37
Figure 4.....	38
Figure 5.....	39
Figure 6.....	40
Figure 7.....	41
Figure 8.....	42
Figure 9.....	43
Figure 10.....	44
Figure 11.....	45
Figure 12.....	46
Figure 13.....	47
Figure 14.....	48
Figure 15.....	49
Figure 16.....	50
Figure 17.....	52
Figure 18.....	55
Figure 19.....	58
Figure 20.....	59

Introduction

The similarities between Earth and Venus in size, bulk density, and composition might suggest that the two planets followed comparable evolutionary paths. This hypothesis could not be tested, however, due to Venus' extreme surface temperatures and thick cloud cover. Once missions started studying the planet, however, the many differences between Earth and Venus became readily apparent. Early studies reveal that Venus hosts a caustic carbon-dioxide rich atmosphere at a constantly balmy 500°C, and has an overall basaltic surface composition. The thick cloud cover around the planet causes minimal diurnal temperature differences, resulting in very weak surface winds. In the early 1990's the National Aeronautics and Space Administration (NASA) launched the Magellan spacecraft to collect gravity, thermal emissivity, and altimetry data as well as synthetic aperture radar (SAR) images. Magellan was to study Venus more comprehensively than any other spacecraft at the time in the hopes that it could shed light on the planets history.

Magellan's altimetry, thermal emissivity, and gravity data provided quantitative data; the SAR images provided a "picture" of the surface of Venus. One landform that stood out in these images is the ever-present impact crater. Impact craters provide a vast amount of information regarding their host's history through size and surface distribution and impact condition. Their spatial distribution in particular provides valuable clues to the relative ages of planet surfaces, and may provide clues to how that planet generates new crust. In general, older surfaces show more impact craters and have a larger average impact crater diameter, indicating that they are less geologically active. Interestingly, Magellan SAR images show that Venus' impact craters are distributed near-randomly

across the surface (Phillips et al., 1992; Strom et al., 1994). Venus lacks large surfaces of statistically distinct ages. In other words, according to the distribution of impact craters, Venus has one statistical age across the surface. This is due to the small number of total impact craters on the surface as well as the relatively narrow range of impact crater diameters. Consequently, impact crater density differences alone are not sufficient to determine the relative ages of surfaces on Venus (McKinnon et al., 1997).

The condition of impact craters can also provide temporal clues, given that older impact craters will appear more modified than their younger, more pristine counter parts. However, of the approximately 975 impact craters on Venus' surface, about 800 are free of volcanic embayment or tectonic deformation (Schaber et al., 1998; Herrick et al., 1997). This is a remarkably low number of modified craters considering the prevalence of volcanic flows on the surface and a highly deformed terrain referred to as tessera that occupies in the highlands, and implies impact crater formation after the volcanic activity ceased. In cases where an impact crater is modified, the modification is more commonly tectonic rather than volcanic (Schaber et al., 1998; Herrick et al., 1997). The low level of modification affecting Venusian impact craters and the near-random spatial distribution of impact craters on Venus are the two main constraints any proposed geologic history of Venus must accommodate.

Given the intrinsic similarities between Venus and Earth, geologists initially considered plate tectonics as the mechanism of Venusian resurfacing. Magellan's altimetry and SAR data show, however, that Venus' surface characteristics are incompatible with the hypothesis of plate tectonics. Venus has unimodal topography (Ford and Pettengill, 1992), suggesting one overall bulk crustal composition, whereas

Earth's oceanic (basaltic) and continental (granitic) crust results in bimodal topography. Venus also lacks global-scale linear features such as mid-ocean ridges, subduction troughs, and linearly distributed volcanoes that are so closely tied to plate tectonics on Earth (Kearey and Vine, 1996). Instead, circular features such as volcanic rises and crustal plateaus dominate Venus' surface (Phillips et al., 1992). Finally, Venus' impact craters are distributed near-randomly across the planet. If plate tectonics operated on Venus, there should be large areas of surface with notably different impact crater densities, indicative of large tracts of young (oceanic) and older (continental) crust. Plate tectonics is clearly not a viable hypothesis for Venesian resurfacing. Subsequently proposed resurfacing hypotheses fall into one of two end-members: catastrophic and equilibrium resurfacing.

Catastrophic resurfacing, which calls for a global resurfacing event that destroyed preexisting impact craters, is the current prevailing resurfacing hypothesis for Venus. This hypothesis easily meets constraint 1. Following global catastrophic resurfacing, resulting in burial of most preexisting impact craters, bolides naturally strike the "post-catastrophe" surface and create impact craters randomly, resulting in a random distribution accumulating on the inactive surface. Because of the low number of modified craters—constraint 2—a stipulation of catastrophic resurfacing is that it must have ended quickly, leaving little record of the transitional phase between flooding and the current low level of geologic activity. Proposed mechanisms of catastrophic resurfacing include widespread volcanic activity (Phillips et al., 1992; Strom et al., 1994) and lithospheric subduction or overturn (McKenzie et al., 1992; Turcotte et al., 1999). However, ongoing geologic mapping and subtle variations in impact crater morphology suggest that Venus

may preserve broad age provinces, however, a discovery that would be inconsistent with catastrophic resurfacing. Although the number and size of impact craters indicates no statistically different surface units, geologic mapping and details of impact crater morphology suggest there may be variations in ages of surface units across Venus.

Equilibrium resurfacing is the other end-member hypothesis for Venus' geologic history (Phillips, 1993; Solomon, 1993). Equilibrium resurfacing incorporates resurfacing in spatially distinct areas—each a fraction of the total surface area—throughout time, destroying pre-existing impact craters and generating new local surfaces after each local event. As in the case of catastrophic resurfacing, possible mechanisms include volcanism or tectonism, albeit on smaller scales. Unlike catastrophic resurfacing, the resulting impact crater distributions do not necessarily meet constraints 1 and 2 simultaneously although both constraints must be met in a time-integrated fashion. Tests of volcanic equilibrium resurfacing using incremental resurfacing areas of 50, 25, and 10% of the total surface area result in a non-random distribution of remaining impact craters (failing constraint 1), whereas similar tests of incremental resurfacing areas 0.03 and 0.003% result in too many modified impact craters (failing constraint 2) (Figure 1) (Strom et al., 1994). These results are called upon as strong evidence against equilibrium resurfacing hypotheses, however resurfacing of areas between 10 and 0.03% were not included. Consequently, equilibrium resurfacing may be viable under these conditions.

In this project, I ran Monte Carlo models on a Venus-sized sphere to more thoroughly test equilibrium resurfacing against the near-random impact crater distribution and low occurrence of modified impact craters. I simulated three resurfacing histories by varying the duration of resurfacing relative to impact crater formation time (1:1, 5:6, and

2:3), specifically focusing on resurfacing increments between 10 and 0.03% of the total surface area. The three resurfacing histories include several experiments, each experiment varying incremental resurfacing values, and each experiment consisting of 1000 test runs to ensure statistical viability. Within each of the resurfacing histories, at least one experiment produced impact crater distributions that met both constraints of Venus' impact crater record. These results indicate that the paradigm of catastrophic resurfacing is not the only possible geologic history consistent with observations of Venus' impact crater record.

Background

- *Venus Background*

Venus lies 1.08×10^8 km from the Sun (0.7219 AU) and has a mass of approximately 5×10^{24} kg (0.8333 times the mass of Earth). Venus' day (243 Earth days) lasts longer than its year (225 Earth days), and the planet undergoes slow retrograde rotation. The atmosphere, which is composed of 96% CO₂, 3.5% N₂, and trace quantities of H₂O, H₂SO₄, HF and HCl, exerts a surface pressure of 95 bars and has a temperature of 470°C. There are three distinct cloud layers within the atmosphere: 0-70 km, 70-110 km, and above 110 km altitude (Lellouch et al., 1997). Winds always blow westward, with upper cloud levels having high wind speeds decreasing with altitude into negligible surface winds (Esposito et al., 1997). Because the surface winds are so weak, they only affect very fine-grained impact sediments, and are not an agent of erosion (Basilevsky et al., 2003; Izenberg et al., 1994; Phillips and Izenberg, 1995; Schaber et al., 1992; Strom et al., 1994). No water currently exists on the surface, and surface compositional analyses from Venera and Magellan SAR images are consistent with a dry basaltic composition (McKenzie et al., 1992; Surkov et al., 1986; McKinnon et al., 1997). Consequently, it is unlikely that there is water trapped in the surface rocks and any erosion on the surface is not likely due to water.

- *Magellan Data Sets*

The NASA Magellan mission collected thermal emissivity, gravity, altimetry, and synthetic aperture radar (SAR) data (Saunders et al., 1992). The altimetry data have a vertical resolution of 80 m and a horizontal resolution of approximately 10 km (Ford et al., 1993). The SAR image resolution is ~120 m/pixel (Saunders et al., 1992).

- *Topography*

Magellan Altimetry data shows that approximately 80% of Venus' surface is within 2 km of topographic relief centered on an average radius of 6052 km, describing a unimodal topography profile (Ford and Pettengill, 1992). In comparison, Earth has a bimodal topography where the most common elevations correspond to the average elevations of oceanic and continental crust. Earth's bimodal topography profile is thus clearly related to plate tectonics and the fundamental differences between continental and oceanic crust, since it is the process of plate tectonics that exploits and reinforces the compositional differences between oceanic and continental crust in order to operate. Because of its unimodal topography profile, Venus' crust cannot be divided into large areas with varying densities, corresponding to compositional variations.

The surface of Venus is divided into three broad topographic provinces, however: the lowlands, mesolands, and highlands. The lowlands and mesolands are morphologically similar, differing in that the lowlands are much more expansive and sit at a planetary radius of 6052 or less. Lowlands have smooth surfaces, called plains or planitiae, with concentrated zones of deformation (Banerdt et al., 1997). Both the lowlands and mesolands are characterized by widespread volcanic flows.

The highlands cover the remaining 10% of the surface and are associated with volcanic rises and crustal plateaus (Figure 2). Volcanic rises are domical features with smooth, flow-like topologies and are thought to result from a current mantle hot spot heating the lithosphere from below (Phillips et al., 1981, 1991; McGill, 1994; Phillips and Hansen, 1994; Smerkar et al., 1997; Nimmo and McKenzie, 1998). Volcanic rises get their name because they are the source of current volcanic activity (Smerkar et al. 1997).

Crustal plateaus, however, are less understood. They are characterized by steep sides and flat tops with tessera terrain cover (Figure 3; Hansen et al., 1999). The tessera terrain atop crustal plateaus is unique to these features and is described by short- and long-wavelength folds cut by short-wavelength fractures (“ribbons”) (Figure 3; Hansen et al., 1999). Ongoing geologic mapping shows outcrops of tessera terrain in Venus’ lowlands, however, suggesting that crustal plateaus may lose their topographic signature over time (Ivanov and Head, 1996; Ghent and Tibuleac, 2002; Hansen et al., 2006). In many cases, the trends of the ribbons and folds conform to the circular patterns, which are also observed on high-standing crustal plateaus, further reinforcing the hypothesis that tessera terrain inliers represent the fossil remains of ancient crustal plateaus. Proposed mechanisms of crustal plateau formation are mantle plumes (Phillips and Hansen, 1998), mantle downwelling (Bindschadler et al., 1992; Bindschadler and Parmentier, 1990; Bindschadler 1995), and impact-induced melting (Hansen, 2006). Each of these hypotheses includes the stipulation that all preexisting structures in the area would be destroyed through the creation of the crustal plateau. There is still debate as to which, if any, mechanism is correct.

- *Impact Craters*

- Morphology

Impact craters on Venus have the same basic morphology as impact craters on other planets and satellites. Venus’ impact craters range in morphology from the typical low-energy bowl-shape depression up to the high-energy multi-ring impact basins (Melosh, 1989). Because there is no water or significant winds on the surface, the impact craters and their associated ejecta blankets are remarkably pristine. Volcanic and tectonic

activities affect some impact craters, but modified impact craters are the exception rather than the norm on the planet. Of Venus' 976 impact craters, only 108 (~11%) are tectonically deformed (faulted, folded) and 56 (~5%) are volcanically modified (embayed) (Herrick et al., 1997; Schaber et al., 1998). Pristine ejecta blankets have blocky and lobate morphologies on the transition zone from the impact crater rim to the surrounding topography (Phillips et al., 1991). Ejecta blanket's scale with the impact crater (McKinnon et al., 1997).

Some impact craters possess an impact crater halo, a feature created by the shock wave interacting with the surface during the impact process. The atmosphere in front of an incoming asteroid becomes compressed as the bolide nears the surface, and when this compressed gas hits the surface it smooths the surface at the impact site. The result is a small area with a different radar character from the surrounding terrain centered on an impact crater. Some halos appear dark compared to the environment while others appear bright (Strom et al., 1994). There are also features referred to as "craterless splotches" which appear to be impact crater halos that formed without the accompanying impact crater. Smaller bolides coming through Venus' atmosphere would burn up too much to impact the surface, but they would still generate the shockwave that would then air-blast the surface (Phillips et al., 1992; Schaber et al., 1992). The final feature to form associated with an impact crater is an impact crater parabola. This is a parabolic shadow formed from the very slight winds blowing the finest-grained material ejected during an impact westward before they fall back to the surface. These features always point to the west since the very weak surface winds always blow to the west (Esposito, 1997). These parabolas are not observed on other planets. Parabolas are only observed on impact

craters larger than 7 km in diameter (Strom et al., 1994), presumably because only impacts that large or larger can eject the finest-grained material far enough into the atmosphere to be affected by the winds. There are approximately 62 (~6-7%) impact craters with parabolas on Venus (Strom et al., 1994).

- Size and Distribution

Venus lacks both large and small impact craters compared to impact crater size distributions on other rocky bodies. Venus' impact craters range in diameter from 1.5 to 270 km and have an average diameter of 20 km (Figure 4) (Herrick et al., 1997; Schaber et al., 1998). In comparison, terrestrial impact crater diameters range from 0.01 to 300 km (Earth Impact Database, 2007), lunar impact craters from 0.001 to 2500 km in diameter (Andersson and Whitaker, 1982), and Martian impact craters between 0.001 to 2300 km in diameter (Cintala et al., 2004; Schultz and Frey, 1990). Venus' exceedingly dense atmosphere is responsible for the skewed distribution of small impact craters; bolides 0.5 to 1 km in diameter undergo significant vaporization while bolides smaller than 0.5 km in diameter burn completely before they reach the surface (McKinnon et al., 1997, Phillips et al., 1992). This interaction between the asteroid and atmosphere prevents the formation of impact craters ≤ 1.5 km in diameter and causes an under-representation of impact craters smaller than 35 km in diameter. Large impact craters (>270 km diameter), on the other end of the spectrum, require relatively large bolides which were much more common in the early solar system. It follows that the lack of these large craters on Venus is not due to the atmosphere but instead either a property preventing impact craters from forming or a planetary resurfacing mechanism responsible for removing large impact craters once formed. Venus is a rocky planet like Mercury, Earth, and Mars—all of which host large

impact crater basins—and there is consequently no justification for saying similar structures would not form on Venus. It reasons, then, that the lack of large impact craters on Venus is a result of a planetary resurfacing process.

Because of the relatively low number of impact craters on the surface, the smallest datable area on Venus is $2 \times 10^7 \text{ km}^2$, or $\sim 4\%$ of the total surface area (Phillips et al., 1992). Venus' 976 total craters and lack of both large and small impact craters indicates an average model surface age (AMSA) of 750 (+350/-400) Ma (McKinnon et al., 1997) and an average impact crater density of ~ 2 impact craters/ 10^6 km^2 . It is critical to note that the AMSA is not an absolute age of Venus' surface but rather an average model age across the entire surface; there could be regions of older and younger surface contributing to this global average model surface age (Figure 5; Hansen and Young, accepted). The error bars, which result from the lack of small impact craters and overall low impact crater density, illustrate the wide range in possible average model surface ages. Additionally, this AMSA incorporates assumptions regarding the bolide flux of the solar system through time, specifically tailored to Venus' conditions (McKinnon et al., 1997). This bolide flux is based on impact crater observations on other terrestrial bodies related to the mass, radius, and location of that body, making it one of the most accurate assessments of the impact crater population of Venus at the current time.

- o Impact-Crater-Based Time Scales

The density and size distribution of impact craters in an area is directly related to the area's age and geological history given a theoretical bolide flux for the planet in question. Older surfaces typically have higher impact crater densities, more degraded impact craters, and a larger average impact crater diameter compared to younger surfaces.

Using this simple relationship, geologists can commonly determine relative ages of surface units using variations in impact crater density. This is a problem on Venus, however, because of: 1) the low overall numbers required for statistical robustness (Campbell, 1999) and 2) the distribution of impact craters is indistinguishable from a random distribution (Hauck et al., 1998; Strom et al., 1994). A near-random impact crater distribution exists at all elevations across the surface as well as across morphologically similar units (Strom et al., 1994). These observations reinforce the conclusion that plate tectonics did not operate on Venus. Plate tectonics keeps specific parts of the crust (in Earth's case, the continental crust) while recycling and regenerating new crust out of the other portions (e.g., oceanic crust). Wind and water have a marked effect of lowering the number of impact craters preserved on terrestrial continental crust. Because Venus lacks wind and water as erosional agents, Venusian plate tectonics would result in easily distinguishable areas of high and low impact crater density across the surface ((even despite the challenges mentioned above), a prediction inconsistent with observations of the planet.

Morphological and deformational variations of impact craters can sometimes define relative ages of units when impact crater density differences alone are not enough. Although Venus has a low number of tectonically and/or volcanically modified impact craters (Schaber et al., 1998; Herrick et al., 1997), small-scale morphological variations can provide clues to determine the relative ages of units. Izenberg et al. (1994) show that impact crater halos lose their bright radar character over time. This is helpful but alone is not sufficient to determine a relative age scale. It also appears that the very fine-grained material comprising an impact craters' parabola is not as resilient to weathering as the

rest of the impact crater. Consequently, impact crater parabolas undergo a predictable degradation sequence with time (Izenberg et al., 1994). As impact craters age, their floors become dark and smoother—if they formed with a parabola—their parabola degrades (Izenberg et al., 1994). Impact crater degradation and impact crater density taken together yield three distinct AMSA provinces (Figure 6; Phillips and Izenberg, 1995; Hansen and Young, accepted). Additionally, many impact craters are shallower than predicted by depth-diameter relationships (Herrick and Sharpton, 2000), and while the exact cause of this possible impact crater floor flooding is unknown, it too appears to be paired with parabola-lacking impact craters. Relatively dull impact craters, or impact craters with radar character similar in intensity to the surrounding area, are generally shallower than their radar-bright counterparts. This shift in radar character corresponds directly to the degradation trends described above.

- *Resurfacing Histories*

Current observations of Venus serve as the first-order constraints on proposed resurfacing histories. These constraints currently stem from two observations of impact craters on Venus: 1) a near random spatial distribution, and 2) a low occurrence of impact crater modification (Phillips et al., 1992, Herrick et al., 1997; Schaber et al., 1998). These are first-order, statistical constraints that, given the lack of quantitative data regarding surface units, impact crater data are the most rigorous way to test hypotheses. This study seeks only to define spatial scales that give statistically possible results, but does not comment on the geologic possibility of such scales. Consequently, I do not attempt to specify a resurfacing mechanism or distinguish between tectonically and volcanically deformed impact craters. Rather, I refer to all impact craters with any style of

modification as “modified impact craters”. This way the results remain as widely applicable as possible for future studies to test the appropriate geology.

Current resurfacing hypotheses fall into one of two end-member cases: catastrophic and equilibrium resurfacing (Figure 7). Catastrophic resurfacing states that the majority of the planet was resurfaced at one time, whereas equilibrium resurfacing entails ongoing localized resurfacing in random areas throughout time. Because lava flows are so prevalent on Venus, tectonism is rarely considered as a mechanism of catastrophic or equilibrium resurfacing.

Catastrophic resurfacing led to a proposed geologic history known as global stratigraphy. In global stratigraphy, 80% of the surface was catastrophically resurfaced approximately at 750 Ma (Basilevsky and Head, 1996; 1998; Basilevsky et al., 1997; Head and Basilevsky, 1998), either via annealing (i.e. Hansen et al., 1999, 2000; Phillips and Hansen 1998; Hansen and Willis 1998) or via lava pond formation due to a large bolide impact inducing localized melting at the surface (Hansen, 2006). Within the context of the global stratigraphy hypothesis, a planet-wide deformation event created all the tessera terrain earlier than 750 Ma, after which the volcanic plains formed during the resurfacing event and were finally affected by impacts to form the impact craters on the surface. Aside from the tessera, the features on the surface represent geologic activity in the last 750 Ma. Global stratigraphy, as well as catastrophic resurfacing, asserts that all impact craters were buried, except those that lay on tessera terrain, within a geologically instantaneous time, in order to ensure there is no record of the transitional phase when geologic activity ceased (Figure 7A). Volcanic resurfacing lasted 10 to 100 million years and ceased within 10 million years (Basilevsky and Head, 1995). Armed with only SAR

images, supporters of global stratigraphy have made drastic assumptions about the three-dimensional nature of the crust through attempts to determine Venus' stratigraphy. Extrapolating two-dimensional surface relationships into the subsurface is equivocal, and there is no geological reasoning to support their conclusions about the relative ages of surface units observed on Venus. Moreover, lava 1-3 km thick is needed to completely cover preexisting structures on the surface. This is in contrast to the evidence that lava flows are thin rather than thick (Lancaster et al., 1995). Alternatively, catastrophic resurfacing operating through tectonism refers to global lithospheric overturn, wherein the old surface is rapidly subducted into the mantle and then a new surface is created (Parmentier and Hess, 1992; Parmentier et al., 1993; Turcotte 1993; Turcotte et al., 1999). There is also no evidence that any subduction occurs on Venus, and is also geologically inconsistent with Venus' impact crater record and unimodal topography profile.

Equilibrium resurfacing, on the other hand, proposes that resurfacing occurred across Venus in increments through time (Figure 7B). As in the case of catastrophic resurfacing, the mechanisms of equilibrium resurfacing could also be volcanic or tectonic. In volcanic equilibrium resurfacing, lava flows would occur at different times across the surface and accumulate to cover preexisting impact craters (Phillips, 1992). Volcanic edifices are widely distributed across the planet so it is possible that volcanic activity could occur nearly everywhere (Crumpler et al., 1997). Equilibrium resurfacing through tectonic processes might be more difficult to envision, however, the format of ribbon tessera terrain might provide a means to locally destroy impact craters through time (Hansen, 2006). This hypothesis has been long discounted for two main reasons: 1)

there are currently only seven high-standing crustal plateaus, and 2) in the eyes of catastrophic resurfacing and global stratigraphy, tessera terrain is the oldest surface on Venus.

Even though tectonic equilibrium resurfacing has not been tested against Venus, volcanic equilibrium resurfacing has. These tests indicate that possible histories of volcanic equilibrium resurfacing are not consistent with observations one and two of Venus' impact crater record. Experiments of equilibrium resurfacing involving resurfacing increments of 50, 25, and 10% of the total surface area produced statistically non-random crater distributions (failing observation one), whereas experiments of equilibrium resurfacing involving resurfacing increments of 0.03 and 0.003% produced too many modified craters (failing observation two) (Figure 1; Strom et al., 1994). There have been no statistical tests of equilibrium resurfacing between 10 and 0.03%, however, so it remains unknown if resurfacing in these areas will show an overlap of impact crater distributions meeting both observations 1 and 2 (Figure 1). It makes sense that as the percent-area of resurfacing increases the resulting impact crater distribution becomes less uniform and the percent of modified impact craters should decrease, because as the resurfaced area becomes larger the circumference-to-area ratio decreases (Figure 8). The problem with previous Monte Carlo models is that they failed to determine where the number of modified impact craters becomes consistent with Venus relative to where the spatial distribution shifts from non-random to near random (Figure 9). Strom et al. (1994) found points X and Y in Figure 9, but failed to find point Z. Without determining if point Z meets or fails *both* constraints one and two, then equilibrium resurfacing is viable on Venus. The previous work did not explore the parameter space necessary to illustrate that

point Z does not exist—such documentation is required to prove that equilibrium resurfacing is not viable. Alternatively, if experiments of parameter space demonstrate that point Z can be achieved, then equilibrium resurfacing is viable. Moreover, the previous Monte Carlo models of equilibrium resurfacing explicitly tested volcanic resurfacing and incorporated assumptions irrelevant for tectonic mechanisms such as the tapering of lava flows and how that will affect the number of modified impact craters observed on the surface. By conducting statistical simulations of equilibrium resurfacing that explore the missing parameter space and consider unspecified resurfacing mechanisms, it is possible to test both volcanic and tectonic modes of equilibrium resurfacing against observations 1 and 2 of Venus' impact crater record. For this reason, I used boundary conditions applicable to both volcanism and tectonism, as to not specify a resurfacing mechanism at the outset.

Methods

This study seeks to test configurations of equilibrium resurfacing (looking at specific percent-area incremental resurfacing and rates of both impact crater formation and resurfacing) against the two key observations of Venus' impact craters—the spatial distribution and overall pristine condition. Because creating and watching the evolution of several thousand Venus-like planets is a logistical nightmare, I ran 1000 Monte Carlo models for each experiment and then statistically analyzed the results. These experiments generated a statistically significant set of impact-crater test statistics, such as inter-crater distances and numbers of modified impact craters, which I could compare to the values observed on Venus. Through this method, it is possible to determine which configurations, if any, of equilibrium resurfacing are consistent with Venus' impact crater record.

- *Monte Carlo Models*

Monte Carlo modeling is a powerful tool used to simulate random processes and processes that are difficult or impossible to observe. Monte Carlo models are statistical models that generate large data sets to give statistically expected results. The models are both useful and necessary because natural systems commonly operate on spatial and temporal scales larger than researchers can reasonably study. Modelers can then compare the statistically expected states of the system to the observations of the natural system in question and determine if the natural system could result from combinations of parameters used in the Monte Carlo models. This methodology can never prove that the Monte Carlo model in question is the only possible configuration to result in the observed system—in fact, the model can only comment on itself and no other possible scenarios—

but by testing a range of configurations it is possible to determine where certain parameters begin to violate the constraints or if a set of parameters could accommodate the constraints.

Monte Carlo experiments operate around a specified probability distribution and corresponding parameters to predict the outcome of natural systems. The experiments in this study specifically utilize the Poisson distribution. Poisson distributions, a widely studied probability distribution, assumes that each spatial and temporal increment has an equal probability of hosting an event and all events happen independently of all other events. An event refers to the occurrence under investigation. It could be the number of cars passing a point on the highway, the speed of birds flying across the country, or an impact crater forming on a planet's surface. Both the resulting spatial distribution of events and the time between events is normal, or Gaussian. Because bolides strike any part of a planet's surface with equal probability and because existing impact craters do not affect the formation of other impact craters, the Poisson distribution is commonly used to model impact cratering processes. By further assuming that resurfacing events occur randomly on the surface, a reasonable simplification in a first-order study, resurfacing processes would then also follow a Poisson probability distribution. With these basic assertions, the viability of equilibrium resurfacing on Venus boils down to the interaction between two competing Poisson processes: one creating impact craters on the surface and another destroying impact craters on the surface. I simulated these two Poisson processes using MatLab Student Version 7.1.

- *Assumptions*

Because Monte Carlo models are simplifications of reality they are always built around a set of assumptions. In this study, the Monte Carlo models incorporated the following six assumptions:

1. Bolides strike anywhere on the surface with (an) equal probability.
2. Resurfacing occurs anywhere on the surface with (an) equal probability.
3. Only resurfacing events remove impact craters from the surface.
4. Craters can be modified an unlimited number of times.
5. Impact craters form at a constant rate.
6. Resurfacing occurs at a constant rate.

The random nature of bolide impacts justifies assumption one. I include assumption two because the hypothesis of equilibrium resurfacing asserts a random nature of resurfacing across the planet. As stated earlier, assumptions one and two together allow modeling of both impact craters and resurfacing events as Poisson distributions. Venus' low surface winds and lack of water geologically support assumption three. Assumption four prevents us from asserting an erroneous limit on impact crater modification and leaves this study as open-ended as possible. Assumptions five and six are merely the logical starting points for this study, and can be changed as better and more accurate information becomes available. Although these assumptions are likely false in detail, both individually and as a set, they are necessary starting points, and form valid first-order assumptions. As the underlying geology and governing physical processes become better understood, new assumptions can be incorporated into the models developed herein to make the models more realistic.

- *Experiments*

Because so little of the underlying resurfacing process is known, I varied both the duration of planetary resurfacing can occur as well as the size of the area resurfaced in one resurfacing event. I used three suites of experiments to isolate and test each variable against a set of purely random impact crater distributions I used as my control set. Each suite has the duration of impact crater formation set at 4.5 billion years (the total age of Venus) with the length of resurfacing varying between 4.5 billion years (Suite A), 3.75 billion years (Suite B), and 3 billion years (Suite C). Impact crater formation and resurfacing fluxes were constant in each experiment, and each experiment consisted of 1000 test runs to ensure statistical viability.

Each suite includes a range of experiments that test multiple values of percent-resurfacing area in order to determine the values that shift the simulations from consistency to inconsistency with respect to each constraint. I used algebraic and geometric series to determine the timing of both impact crater formation events as well as the length of time between resurfacing events using the constraints of an average of 100 percent total resurfacing and 1000 final impact craters on the surface (Appendix I). These calculated fluxes serve as Poisson means in a given experiment, and the calculated length of time between resurfacing events and impact crater formation events used in each time scale is normally distributed around these means.

All of the test runs in each experiment with each of the three suites followed the same procedure. The sequences of independent, randomly generated intervals between impact crater formation and resurfacing events serve as the timescale for the test run. Summing the number of impact craters formed between resurfacing events gives the

number of impact craters created in that time step (Figure 10). Each test run has a unique time scale. Spatially random locations for impact craters and the centers of resurfacing events are generated for each impact crater and resurfacing event in the test run. The number, location, and condition of impact craters are tracked as outputs of the model (Figure 11). A sample script for a test run is given in Appendix II. An impact crater can be in one of three possible conditions after a resurfacing event (Fig. 12): (1) pristine—the impact crater lies more than R_a+2R_c from the center of the resurfaced area, (2) modified—the impact crater is between R_a+2R_c and R_a-2R_c from the center of the resurfaced area, and (3) destroyed—the impact crater lies less than R_a-2R_c from the center of the resurfaced area. Following assumption four, there is no limit on the number of times an impact crater can be modified by resurfacing events. This leads to the motivation for tracking the number of modified impact craters and the number of modification events for individual impact craters. If impact craters in the experiments are undergoing several (three or more) modification events, it is more likely that in actuality those impact craters would be unrecognizable on the surface. Such a result would lower the number of modified impact craters expected in that experiment. Because there is no limit in this study, it is possible to determine if impact craters are modified multiple times, and therefore to be able to determine if it is unreasonable to assume that impact craters would be identifiable structures, and, in this case, reassess the expected number of modified impact craters in each experiment.

Several statistical tests exist to determine the randomness of spatial distributions; two tests were utilized for this research. The first test compares the distribution of intercrater angles to the theoretical relationship

$$f(\alpha) = M \cdot \sin(\alpha),$$

where M is a scaling factor, and α is the angle between two impact craters measured from the planet's center (Figure 13; Kagan and Knopoff, 1980; Turcotte et al., 1999). For N impact craters, there are $[N \cdot (N-1)/2]$ intercrater angles. Given that there are on average 1,000 impact craters at the end of each test run, the expected number of intercrater angles is $999 \cdot 500$, or 499,500. This is clearly a large number. These roughly half-a-million data points were sorted into equal-sized bins to create a meaningful frequency histogram. Because using too many or too few bins will obscure the analysis by either adding unnecessary noise to the plot or smearing over significant variations, I followed the procedure of Turcotte et al. (1999) to sort the data into thirty-six bins for analysis. To find the theoretical curve, I set the variable (α) equal to the midpoint of each bin and calculated $f(\alpha)$. To find M , I summed the area in each bin of the histogram in the experimental results and divided this by the integral of $f(\alpha)$ (Appendix III). Any clumping in the impact crater distributions would show in the frequency histogram as a bump of intercrater angles above or below the theoretical curve. To quantify the correlation between shifts in the observed and theoretical variations in intercrater angles, I calculated the R^2 value between the observed and expected curve for each test run. An R^2 value close to 1 indicates a good correlation between the theoretical and observed relationships, in this case indicating a more random surficial distribution, whereas lower R^2 values indicate a weaker correlation between the two curves.

The second, more sensitive statistical test quantifies the spherical randomness of the simulated impact crater distributions directly by comparing the amount of clumping in experimental and control simulations. A measure of clumping in the impact crater

surface positions is the “resultant vector”, the sum of the vectors of each individual impact crater, where the randomly generated (x, y, z) coordinates serve as the head of the vector and the origin (0,0,0) is the tail (Figure 14). A concentration of impact craters on the surface is characterized by a longer than expected resultant vector compared to a purely random distribution. The location of this overall clump is not meaningful except as a check that the impact cratering process was indeed random. Rather, it is the magnitude (length) that is a useful measure of clumping on the surface. Because even purely random distributions will have some clumping, I compared the length of the resultant vector in each experiment to purely random simulations, as well as to the distribution of Venus’ documented impact craters. In comparing the resultant vectors of experimental and control-simulated distributions, I calculate the mean and standard deviation in each experiment and used the chi-squared test to statistically determine if the same process could give rise to both distributions. The chi-squared test directly measures statistical similarities between random and simulated distributions and consequently is well-suited for this task (Strom et al., 1994; Walpole et al., 2007). I also used the more basic method of comparing the mean and 95% confidence intervals for the magnitude of resultant vectors in both the random and experimental distributions to check for overlaps. If the confidence interval for each experiment overlaps with the confidence interval for a purely random simulation, then the two data sets are statistically indistinguishable, and the surficial distribution of impact craters in the resurfaced experiment cannot be distinguished from random (Glaze et al., 2002). This method does not work to compare impact craters on Venus, however, because on Venus there is only one data point and no confidence interval. To compare the resultant vectors of experimental distributions to

Venus, I determined if the magnitude of Venus' resultant vector falls within the 95% confidence interval for the resultant vector magnitude for each experimental and randomly simulated distribution. In this way, I ensure that not only is the randomness of each distribution quantified but also the experimental distributions correlate to Venus.

To test constraint two—the number of modified craters—in simulated impact crater distributions against the impact craters on Venus, I followed the same method used to compare the resultant vectors between simulated impact crater distributions and the impact crater distribution on Venus. I calculated the mean and standard deviation of the number of modified craters in each experiment, and determined where the number of modified craters on Venus falls relative to this interval. This approach allows for three possible outcomes: the number of modified impact craters on Venus are 1) greater than the upper limit, 2) fewer than the lower limit, or 3) within the confidence interval for an experiment. Of these, the only case where an experiment fails to meet constraint two is case two, where Venus has fewer than the lower boundary of the confidence interval of that experiment (Figure 15). Because the number of modified impact craters on Venus serves as an upper limit, it is not a problem if this is higher than the number predicted by an experiment.

Results

Experiments in each suite defined the boundaries for both constraints being tested. In other words, experimental results showed a transition from a parameter space where impact crater distributions were statistically near-random but created too many modified impact craters (failing constraint 2, meeting constraint 1) to where the surficial distribution of impact craters was clearly non-random but the number of modified impact craters was low enough to be consistent with Venus (failing constraint 1, meeting constraint 2). I was able to determine which, if any, percent-resurfacing areas could meet both constraints of Venus' impact crater record, and how that window of possible values changes as a function of the length of resurfacing time.

The results of the Monte Carlo models were consistent with expectations yet also reveal surprises. As expected, variations in both percent-resurfaced area as well as the duration of resurfacing affected the resulting impact crater distributions. Table 1 summarizes the results of each experiment, and Figure 15 graphically shows which experiments resulted in final impact crater distributions with a low enough number of modified impact craters to remain consistent with Venus. The near-random surface distribution proved to be the harder constraint to meet than the low number of modified impact craters. Suites B and C, in which resurfacing ended prior to the end of the test runs, include more experiments resulting in random final crater distributions, or more experiments that met the spatial constraint. This confirmed the intuitive conclusion that the longer impact craters are allowed to form on the surface without the effects of resurfacing (removal), the more random the resulting distribution. Additionally, the R^2 test of spatial randomness between the experimental and calculated curves proved to be

less sensitive than the resultant vector test. The analysis was complicated because Venus' impact crater distribution is not purely random. The analysis had to take into account that simulated distributions could fail against random distributions but still be indistinguishable from Venus. For this reason, Table 1 includes tests comparing experimental impact crater distributions against both the purely random simulations and Venus. If an experiment is non-random but is consistent with Venus, it meets constraint one.

Suite A, wherein impact crater formation and resurfacing occur throughout the entire test run, had the fewest number of experiments that met both constraints 1 and 2. Only one experiment—resurfacing in increments of 0.1% total surface area—met both constraints. This is a particularly interesting result in that 0.1% is 1/1000th of the total surface area, and the experiments had a constraint of 1000 final impact craters on the surface. In this way, it is almost intuitive that resurfacing in amounts equal to the “personal space” of each impact crater will maintain the near-random surface distribution. When resurfacing is in 0.1% of the total surface area, there will be one impact crater destroyed (on average) in each time step and one impact crater emplaced before the following the resurfacing event. In other words, the steady-state resurfacing scenario does indeed maintain the original near-random surface distribution, maintaining the steady state. According to the R^2 test, all experiments except 10% resurfacing resulted in spatially random impact crater distributions. This is misleading, however, because many of these final impact crater distributions are non-random simply by visual inspection. The 0.1% resurfacing experiment fails the resultant vector test by a slim margin, and consequently there is a blurry line as to whether the final impact crater

distributions in this experiment are statistically random. None of these experiments is statistically random, and it is only after comparing them directly to Venus that any of the results meet the constraints. This suite of experiments clearly shows how crucial it is to compare simulated impact crater distributions directly to Venus. Figure 16 shows four resulting impact crater distributions from each experiment in Suite A.

In Suite B, where resurfacing occurred only during the first 3.75 billion years of the test runs, only 0.1% incremental resurfacing met both constraints. According to the R^2 test, every experiment included in this suite (up to 50% resurfacing) resulted in spatially random distributions (Table 1). This is again misleading and shows that the R^2 test is not discerning enough to determine which distributions are indeed random. Figure 17 shows sample distributions of impact craters remaining on the surface from each experiment.

Suite C, in which both resurfacing and impact crater formation take place for the first 3 billion years and impact crater formation continues alone for the last 1.5 billion years, had the highest number of experiments that met both constraints of Venus' impact crater record. Incremental resurfacing in 1, 0.7, and 0.1% of the total surface area all resulted in a near random surficial distribution and low number of modified impact craters. Of these, only resurfacing in 0.1% is consistent with a purely random distribution with the other two experiments being only random enough to match Venus' impact crater distribution. Figure 18 shows the spatial distribution of craters remaining on the surface from several test runs in each experiment.

Discussion

These new Monte Carlo models show that certain configurations of equilibrium resurfacing can in fact meet the low number of modified impact craters and their near-random surficial distribution observed in Venus' impact crater record. The number of possible configurations depends on how long resurfacing occurs in the test run. The experiments with the shortest duration of resurfacing, Suite C, contained the largest number of statistically possible equilibrium resurfacing histories. In the case that resurfacing is allowed to continue for the entire test run, the number of possible equilibrium resurfacing possibilities shrink considerably. This result is somewhat intuitive, because termination of resurfacing processes earlier in a planet's history would provide more time for impact craters to smooth out any clumping caused by localized resurfacing.

Because a study similar to this study already exists (Strom et al., 1994), analogous models were crucial to establish credibility and allow for direct comparison of results. Suite A has the same boundary conditions as the Monte Carlo models of Strom et al. (1994), and consequently serves as the direct link between the studies. Suite A is the most basic study and considers equilibrium resurfacing when both impact crater formation and resurfacing occur at constant rates throughout the entire test run. Strom et al. (1994) ran the original models and purportedly tested volcanic equilibrium resurfacing. They found that of the various resurfaced areas they tested, only tests of 100% resurfacing produced results matching the observations of Venus' impact crater record (Figure 1). This is because the number of modified craters becomes too large for resurfacing smaller than 0.1%, and the resulting crater distributions are too non-random for resurfacing in areas

larger than 0.1% to reconcile with Venus. Suite A reached the same conclusions for the percent-area tested, but it differs from the original assertion of catastrophic resurfacing as the only configuration consistent with impact craters on Venus by testing the percent-area between 10 and 0.03%. By including these incremental resurfacing areas, it becomes apparent that catastrophic resurfacing is not the only possible resurfacing area for Venus' geologic history. Resurfacing in 0.1% of the total surface area meets both constraints, and as such, is viable, even in the most basic formulation (Figure 19). This alone is enough to justify further research regarding equilibrium resurfacing and its applicability to Venus.

Because one of the geologic constraints is the low number of modified impact craters, it is imperative to understand what the statistics tracked in these test runs actually means. The total number of modified impact craters reported in each test run is a good approximation of how many deformed, but recognizable, impact craters would exist on the surface under a given set of experimental conditions. There is a caveat, however, because there is no modification limit after which a crater is "destroyed", as there was in the Strom et al. (1994) analysis. If a low number of craters are experiencing the majority of modification, then the number of reasonably observable modified craters is much less than the total number of modified craters reported by the simulations. Except in the case of 0.1 and 0.01% resurfacing, most modified craters undergo a single modification event (Figure 20). Therefore, there would be little deviation between the total number of modified impact craters and the number of recognizable modified impact craters. Even if impact craters underwent many modification events in the test runs, the number of modified craters reported are the maximum number, and would only affect the

comparison of simulated impact craters with impact craters on Venus by reducing the total number of craters on the surface.

The spatial distribution is central to the equilibrium resurfacing debate, so the statistical analysis included two tests to independently quantify randomness within resulting impact craters' distributions. The first test involved finding all intercrater angles, binning these in increments of $0.05 \cdot R$, and quantifying the fit between this line and the same curve of a purely random distribution. Suspiciously, this test only failed one experiment: Suite A, with 10% resurfacing. Even with the reduced amounts of resurfacing in Suites B and C, these test runs should intuitively still create non-random final impact crater distributions for the larger percent-area resurfacing experiments—experiments up to 50% resurfacing reported “random distributions”. Through the second resultant vector test, however, it becomes apparent that several impact crater distributions that the first test deemed spatially random are, in fact, non-random and consequently do not match Venus' impact crater distribution. Additionally, even visually random impact crater distributions failed against the sensitive resultant-vector test, emphasizing the importance of quantifying the randomness in these experiments. With the very narrow range of statistically possible experiments reported by the resultant vector test, these results represent a minimum of possible configurations.

Although the discovery of impact crater data sets resulting from 0.1% resurfacing in Suite A is consistent with the distribution and condition of impact craters on Venus, there are many reasons to look at the effects of other constraints such as the duration of resurfacing in a test run. Suite A, with both resurfacing and impact crater formation for the entire duration of the test run, is the simplest model and is also geologically

unrealistic. It is well established that a higher number of asteroids crossed the orbits of other planets at the start of the solar system and during the late heavy bombardment, resulting in an exponentially decreasing frequency of impact crater formation as the solar system ages (Culler et al., 2000). The average size of impactors has also decreased through time, resulting in fewer impacts with the ability to generate multi-ring impact craters, impact basins, and impact-generated melting. These effects of variable impact crater rate and size were not considered in this first-order study.

In addition to the variable resurfacing rate throughout time, Suite A is also unrealistic due to the assumptions of resurfacing throughout a planets' lifetime. Venus' heat loss is occurring at a very different rate today than it was earlier in its history, due to both the decreasing heat budget and the thickening of the lithosphere. Imposing a constant resurfacing rate throughout a test run effectively ignores this change throughout a planet's lifetime, and a decreasing resurfacing rate, ideally exponentially, is much better suited to approximate this behavior. Although they still impose constant rates of impact crater formation and resurfacing, Suites B and C reflect the shift to a Venus too cold to undergo resurfacing and are consequently more geologically reasonable. Additionally, the imposition of 100% total resurfacing has no geologic basis and arises from a need to start the experiments somewhere. Were this total percent-resurfaced smaller, one would expect fewer modified impact craters (fewer resurfacing events), and more modified impact craters of the total percent resurfacing was higher than 100% (more resurfacing events). Those effects could and should be incorporated into more sophisticated models based on ongoing geologic mapping results.

Conclusion

By looking at several suites of experiments to test the effects of shortening the resurfacing time and employing several statistical tests in my analysis, this study was able to achieve a more complete and rigorous assessment of equilibrium resurfacing and its applicability to Venus. These models clearly indicate that there exist possible configurations of equilibrium resurfacing that replicates the two first-order observations of impact craters on Venus, even under the strictest of resurfacing histories (Suite A). Suite A does not, however, produce a statistically random impact crater distribution but rather a distribution that is consistent with impact craters on Venus. This highlights the importance of comparing the simulated final impact crater distributions directly to Venus and not simply to a random population. As a set, the three suites of experiments surpass the basic model to include a variety of resurfacing histories by varying the duration of resurfacing in each suite and determining how this affects the number of possible equilibrium resurfacing configurations. These models thus become more realistic and show that many configurations of equilibrium resurfacing are potentially statistically consistent with Venusian geology. As the duration of resurfacing decreases, the number of possible resurfacing histories increases, indicating a wider range of possible experiments. The assumptions of constant impact crater formation and resurfacing rates are simplifications but do not detract from the conclusions because this is a first-order study. The next step is to incorporate a more complex, geologically reasonable resurfacing and impact crater formation fluxes into these models and statistically test which configurations of both catastrophic and equilibrium resurfacing are then consistent with the geology of Venus.

The question of Venusian resurfacing is complex and requires much more work before it will be fully understood. The only way to further discern between possible resurfacing mechanisms, both within the dichotomy of catastrophic and equilibrium resurfacing as well as other frameworks not yet proposed, is to continue to map the surface in detail, determine geologically-based tests of all possible hypotheses, and continue thinking outside the box. Venus is clearly a rich planet with a very different history than Earth and sorely needs more work to understand its rich history.

Summary of Results

	Data				Meets Constraint?			
	Area	R ²	Vector Sum	Num Modified Craters	R ²	Vector Sum vs Random	Vector Sum vs Venus	Few Modified Craters
Test A	10	0.905	152.9	14	No	No	No	Yes
	5	0.938	112.9	19	Yes	No	No	Yes
	1	0.965	57.3	41	Yes	No	No	Yes
	0.7	0.969	50.8	48	Yes	No	No	Yes
	0.1	0.981	33.2	130	Yes	No	Yes	Yes
	0.01	1.000	30.8	719	Yes	Yes	Yes	No
Test B	50	1.000	160.9	5	Yes	No	No	Yes
	25	0.961	167.6	9	Yes	No	No	Yes
	20	0.949	155.9	10	Yes	No	No	Yes
	10	0.943	118.0	14	Yes	No	No	Yes
	5	0.955	86.2	20	Yes	No	No	Yes
	1	0.987	46.6	45	Yes	No	No	Yes
	0.1	0.999	31.9	150	Yes	No	Yes	Yes
	0.01	1.000	29.4	547	Yes	Yes	Yes	No
Test C	50	1.000	107.9	4	Yes	No	No	Yes
	25	0.975	121.1	6	Yes	No	No	Yes
	20	0.972	95.6	6	Yes	No	No	Yes
	10	0.968	86.9	7	Yes	No	No	Yes
	5	0.970	66.5	10	Yes	No	No	Yes
	1	0.979	39.7	23	Yes	No	Yes	Yes
	0.7	0.979	37.0	27	Yes	No	Yes	Yes
	0.1	0.983	30.6	71	Yes	Yes	Yes	Yes
	0.01	0.999	28.6	401	Yes	Yes	Yes	No
Random	1	29.5	N/A	Yes	Yes	N/A	N/A	
Venus	0.995	40.5	170	N/A	N/A	N/A	N/A	

Not Possible
Specific Test Failed
Possible

Key:

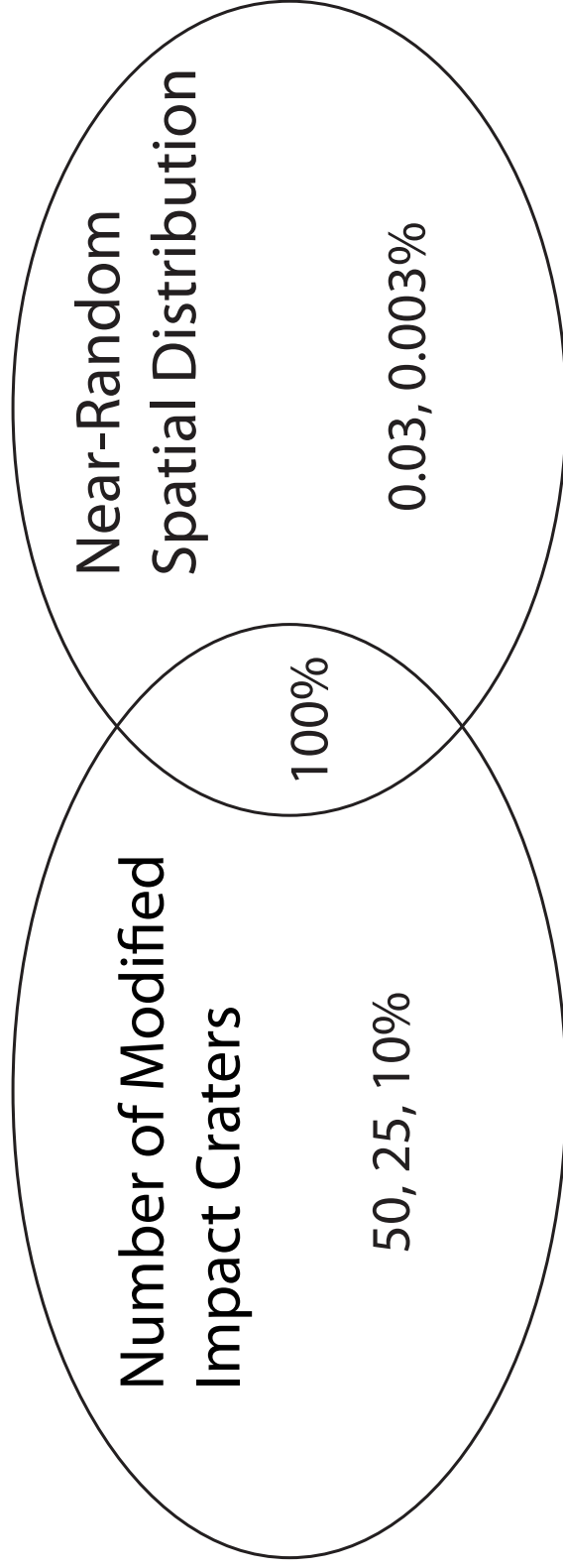


Figure 1: Venn diagram showing the results of Strom et al. (1994). The only resurfacing area they tested which met both constraints of Venus' impact crater record was 100%, or catastrophic resurfacing. All resurfacing areas that they tested are included.

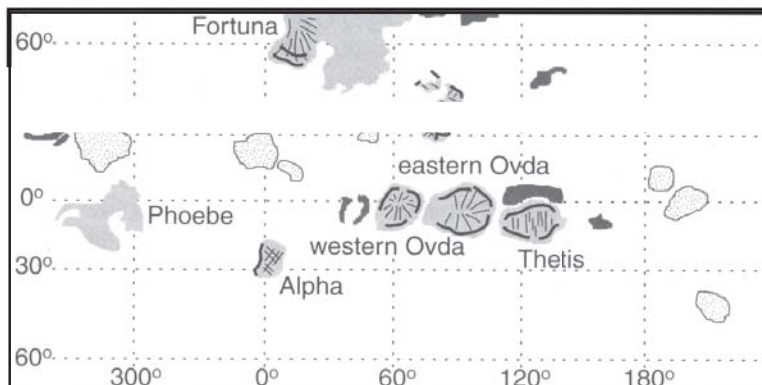


Figure 2: Map outlining volcanic rises and crustal plateaus on Venus. Outlined white areas represent volcanic rises and gray areas represent crustal plateaus, with thin lines following the trends of ribbons and the thick lines following the trends of folds within the tessera terrain. After Hansen et al. (1999).

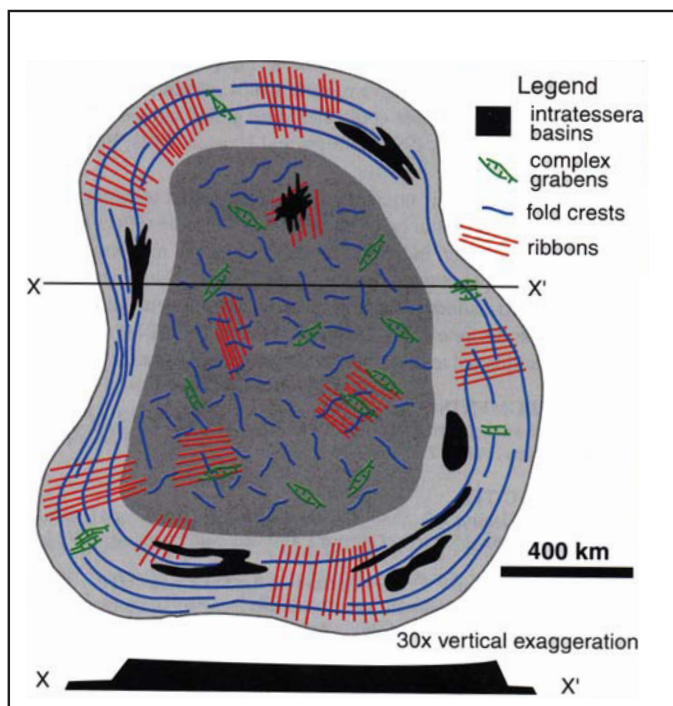


Figure 3: Schematic structural features of crustal plateaus. Folds and ribbons are orthogonal, and the sides of crustal plateaus are nearly vertical. After Hansen et al. (1999).

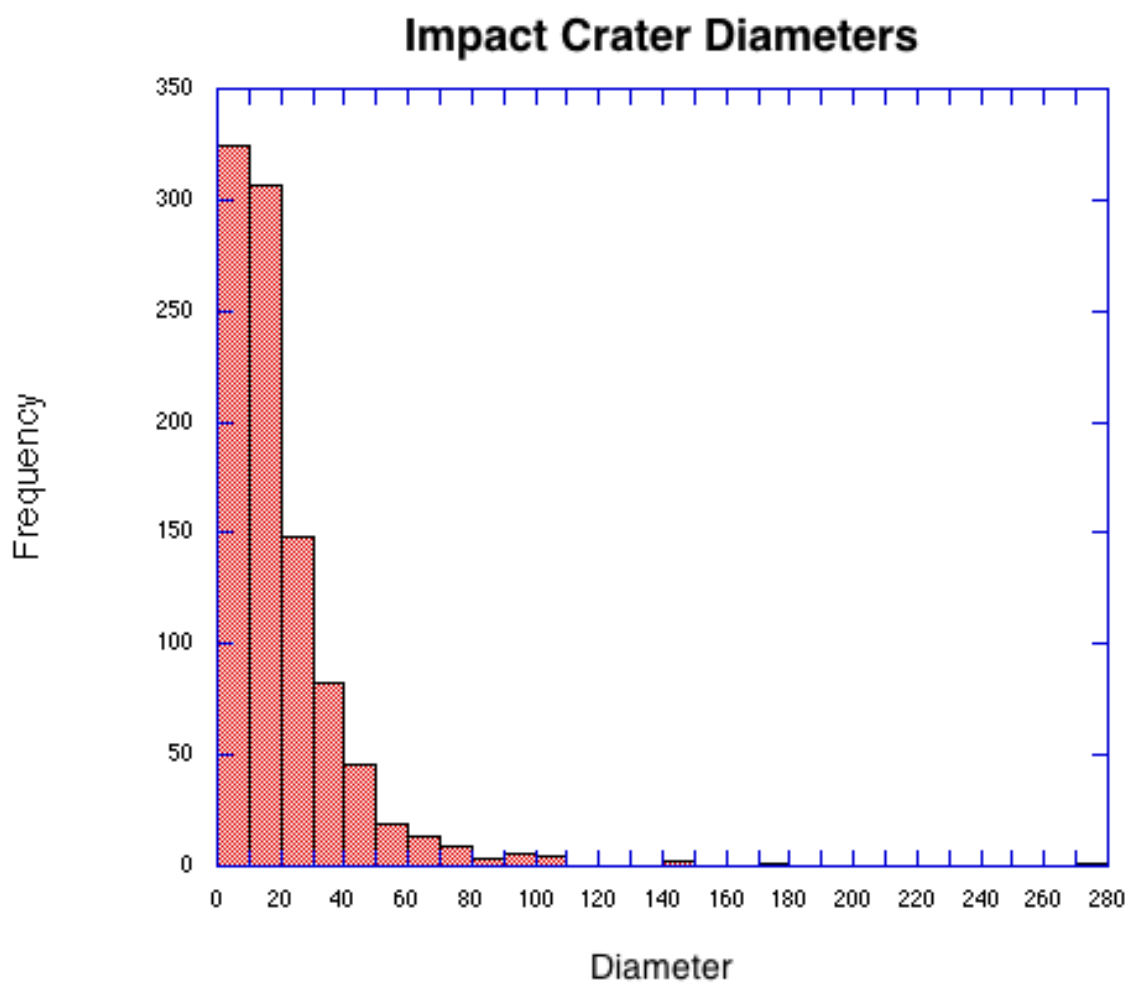


Figure 4: Histogram of impact crater diameters on Venus. The distribution is clearly skewed to smaller diameters, making the median diameter smaller than the average diameter of impact craters on Venus.

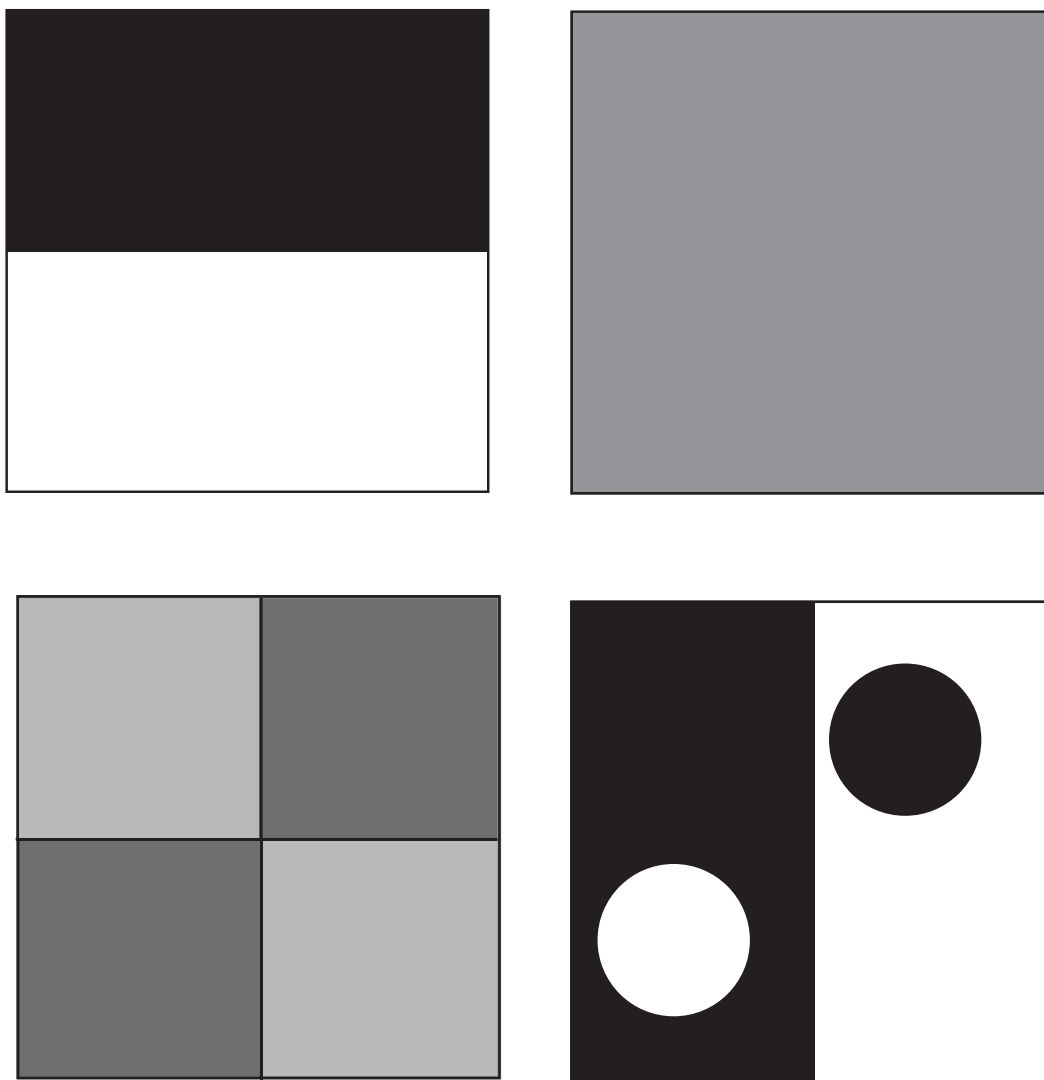


Figure 5: Four different configurations of black and white boxes which have an average 50% grayscale value. Clearly the histories which would give rise to each distribution of grayscale values is vastly different, and the simple fact that they each have an average grayscale value of 50% is not enough to say that they are not significantly different.

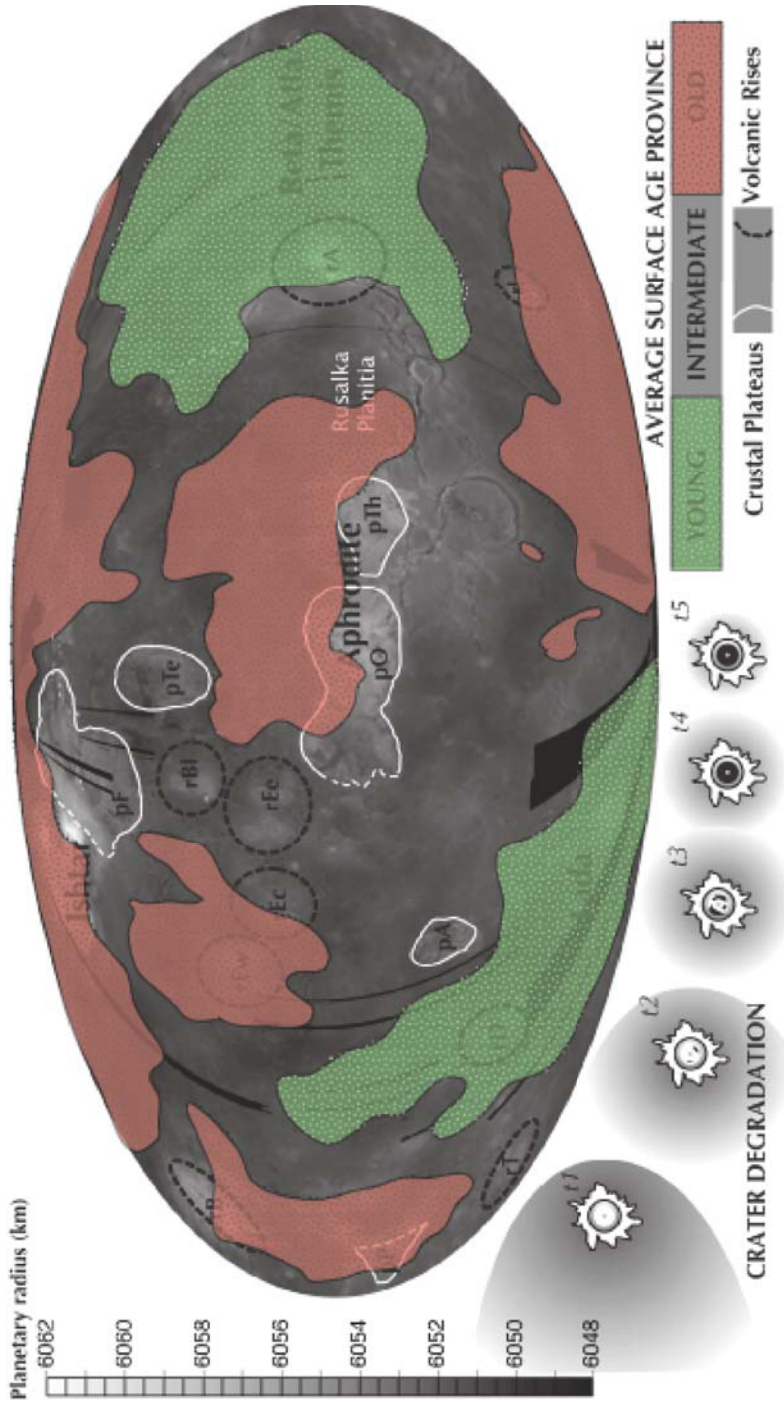


Figure 6: Global distribution of the three age provinces on Venus, determined by small-scale variations in impact crater distribution and morphology. The green areas represent the youngest surface, gray areas represent the oldest surfaces on the planet. Underlying gray-scale variations correspond to elevation differences across the planet in accordance with the left side. The impact crater degradation sequence at the bottom shows the progression of impact crater morphologies as they age. As an impact crater ages, it loses its parabola and the interior floor darkens. Crustal plateaus are outlined in white lines and volcanic rises are outlined in dashed black lines.

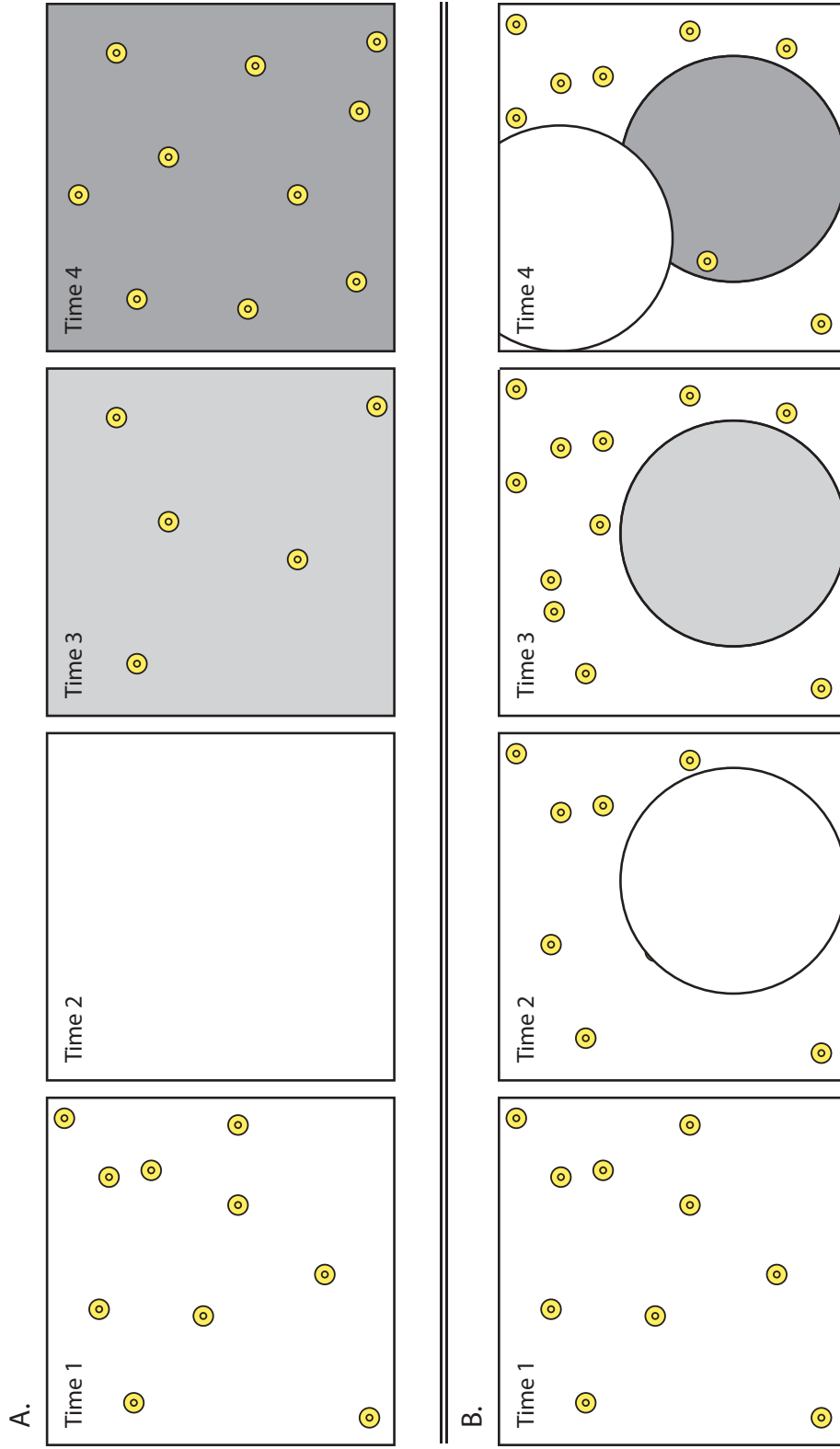


Figure 7: Two time scales showing the fundamental differences between catastrophic resurfacing (Part A) and equilibrium resurfacing (Part B). Resurfaced areas first appear as white areas which transition to darker shades of gray as time passes. Whereas catastrophic resurfacing affects the entire surface at once, equilibrium resurfacing allows for the possibility that some areas of the surface were never resurfaced at all and others were resurfaced more than once.

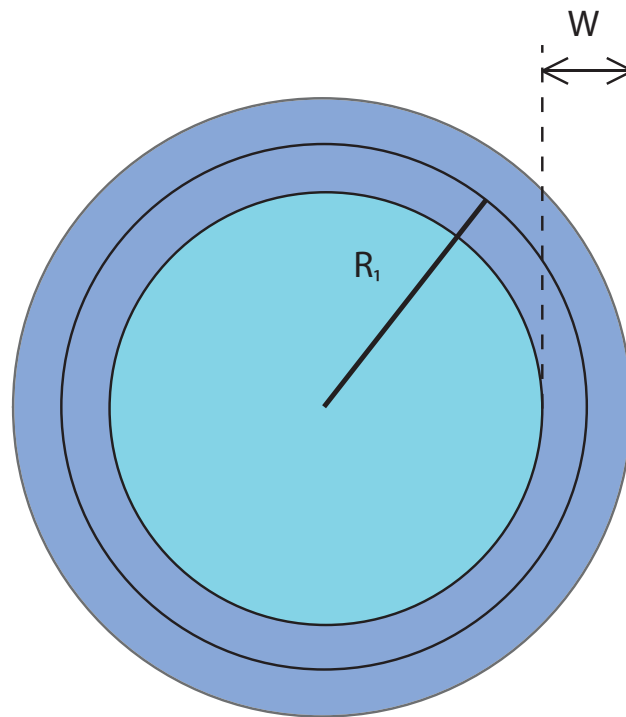


Figure 8: Cartoon illustrating the relationship between where impact craters are destroyed (light blue) and modified (dark blue). The area where impact craters are destroyed is equal to $\pi(R_1 - W/2)^2$ and scales as R_1^2 , with R_1 being the radius of the resurfaced area. This is much higher than how the area of the impact crater modification zone grows, with this zone being defined as the area $2\pi R_1 W$. This area scales as R_1 , and consequently does not grow nearly as fast as the area wherein impact craters are destroyed. This difference is responsible for the fact that as resurfacing areas increase in size, the number of destroyed impact craters grows faster than the number of modified impact craters.

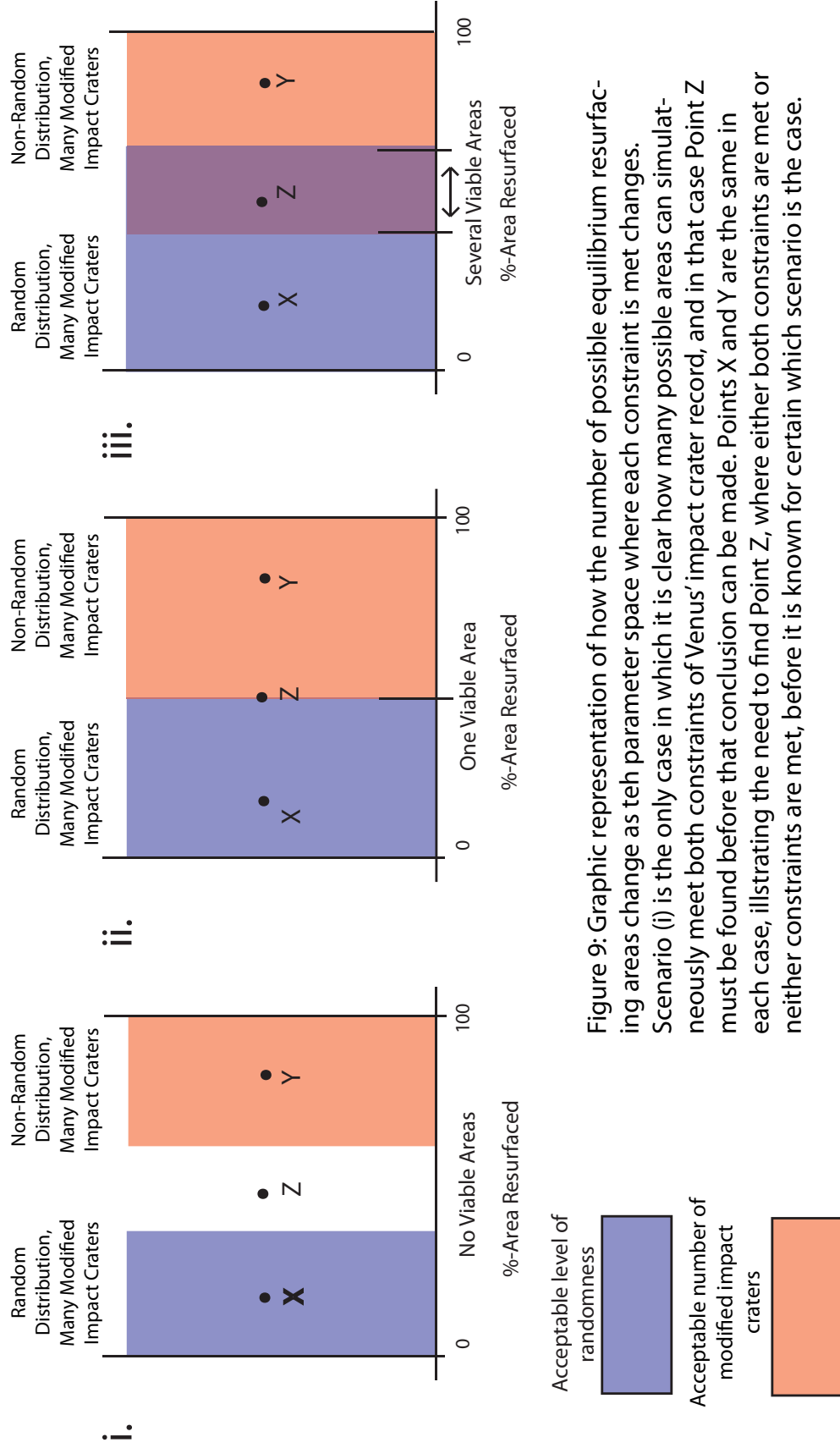


Figure 9: Graphic representation of how the number of possible equilibrium resurfacing areas change as the parameter space where each constraint is met changes. Scenario (i) is the only case in which it is clear how many possible areas can simultaneously meet both constraints of Venus' impact crater record, and in that case Point Z must be found before that conclusion can be made. Points X and Y are the same in each case, illustrating the need to find Point Z, where either both constraints are met or neither constraints are met, before it is known for certain which scenario is the case.

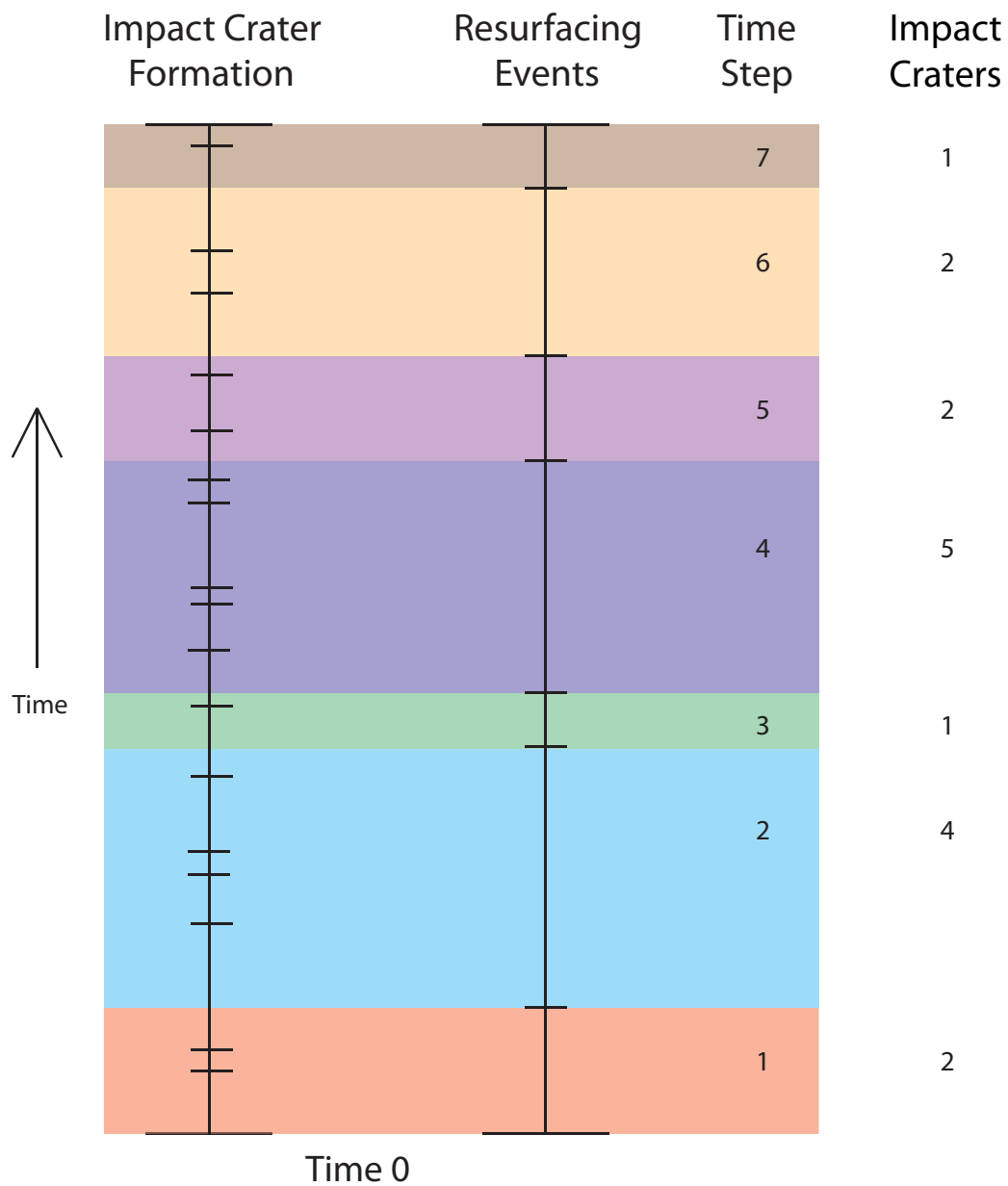
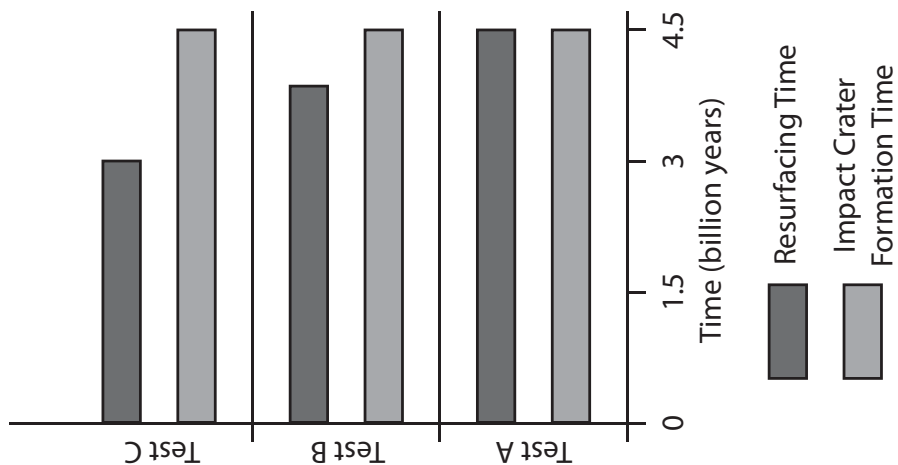
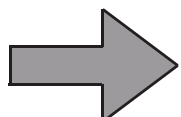


Figure 10: Schematic time scale set up in a typical experiment. Duration between impact cratering events and resurfacing events are independently generated, and the number of impact craters formed between resurfacing events is counted.



1000 Test Runs
 1000 Avg Craters
 100% Avg Resurfacing



Impact Crater Locations
 Number of Modified Craters
 Number of Modification Events

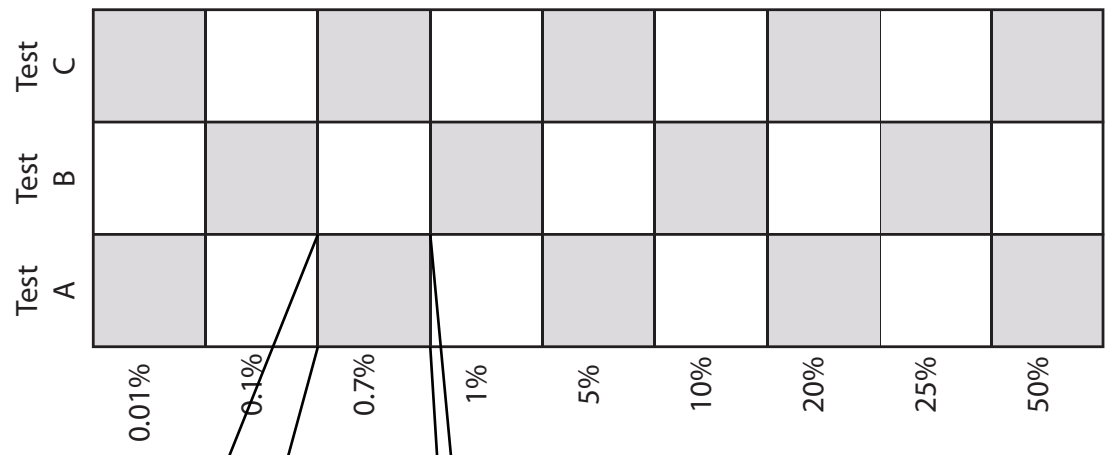


Figure 11: Experimental setup in terms of configurations of experiments within each suite and model inputs and outputs

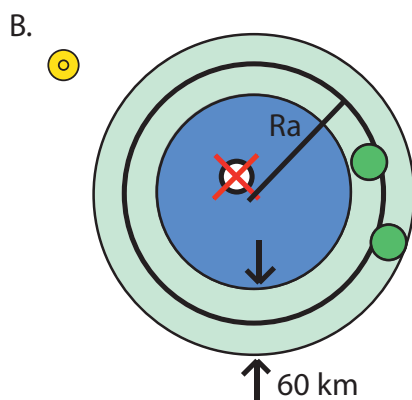
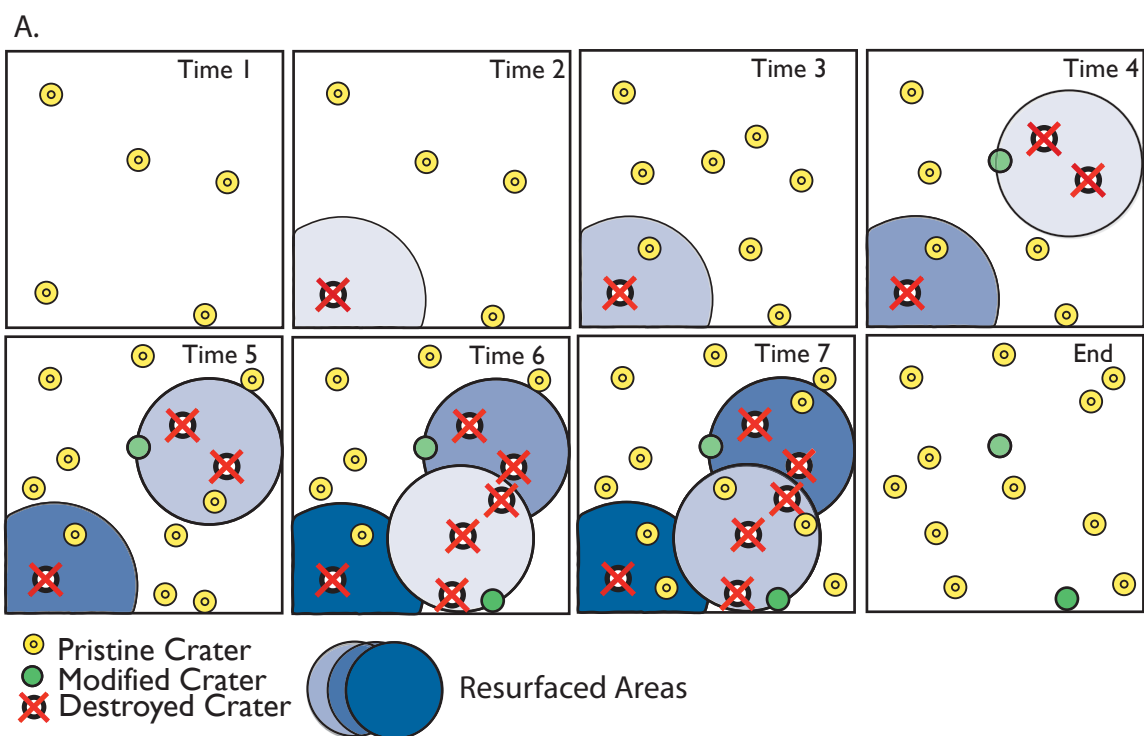
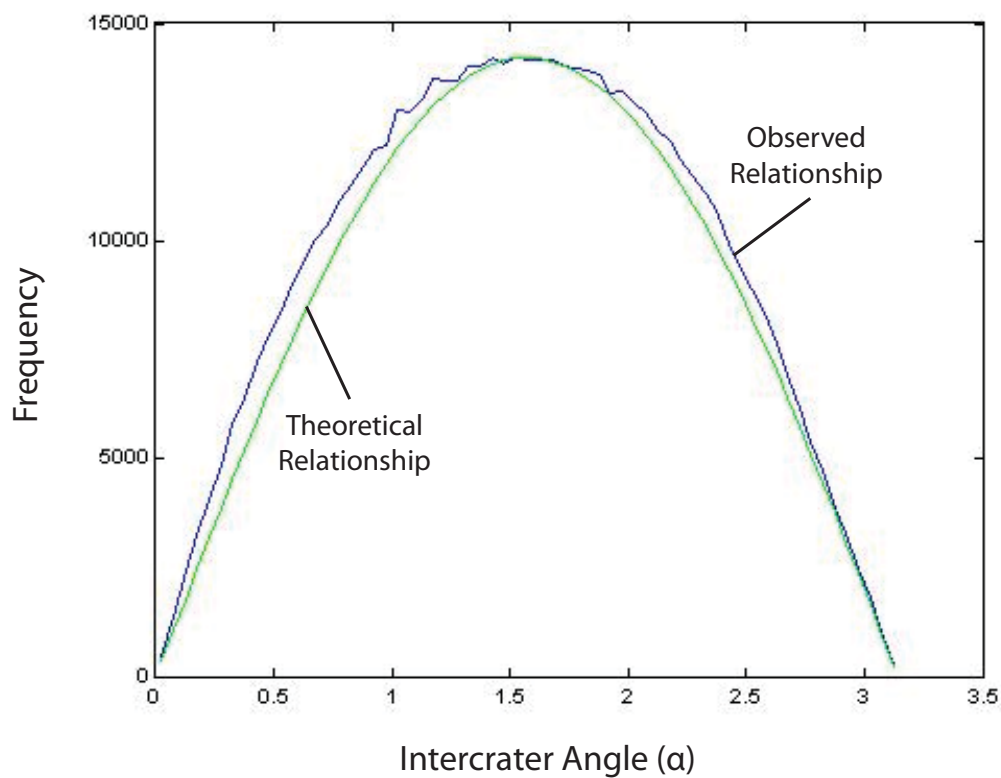


Figure 12:

A) Cartoon of time steps in each test run and how they affect impact craters on the surface. Destroyed and modified impact craters are carried through each time step, and the complexity of the distribution of pristine, modified, and destroyed impact craters is shown in Time 7. The last panel represents what the actual end distribution would show--two modified impact craters and eleven pristine impact craters left on the surface.

B) Close-up on a crustal plateau and the areas which produce the three types of post-resurfacing impact craters (pristine, modified, and destroyed). The width of the anulus surrounding the crustal plateau is held constant in all experiments at 60 km, taking the average radius of an impact crater on Venus to be 30 km.

A.



B.

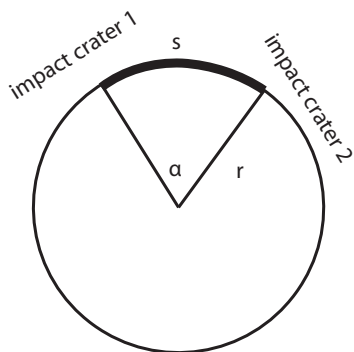
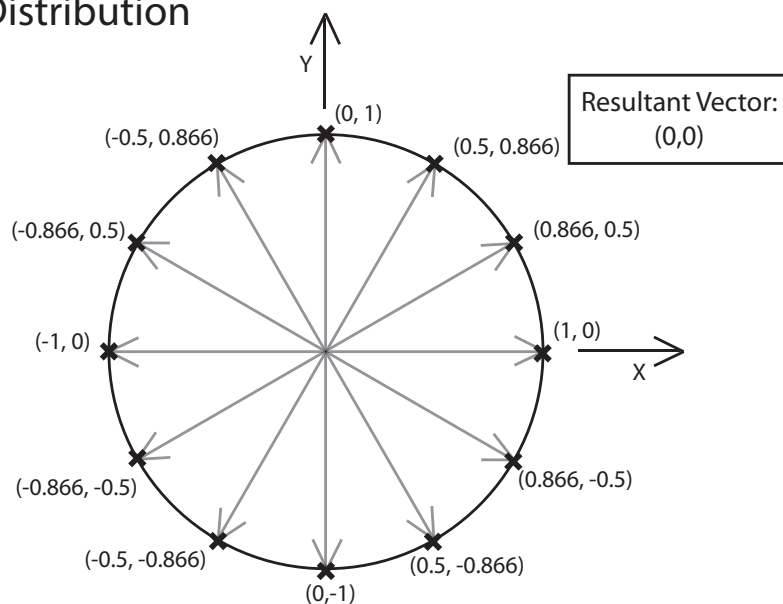


Figure 13: Sample graph illustrating the relationship between an experimentally observed distribution of inter-crater angles relative to a theoretical distribution. To the side (B) is a cartoon showing the geometry of how an inter-crater angle is defined.

A.

Uniform Distribution



B.

Random Distribution

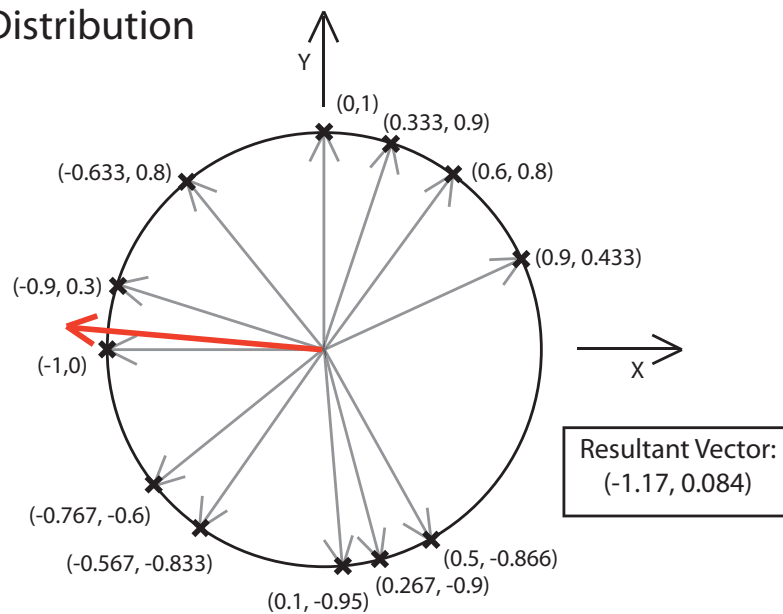


Figure 14: Cartoon illustrating the theory of resultant vectors. The resultant vector of a random distribution is shown in red, and the more skewed the distribution becomes the larger the magnitude of the resultant vector will be.

Modified Impact Craters

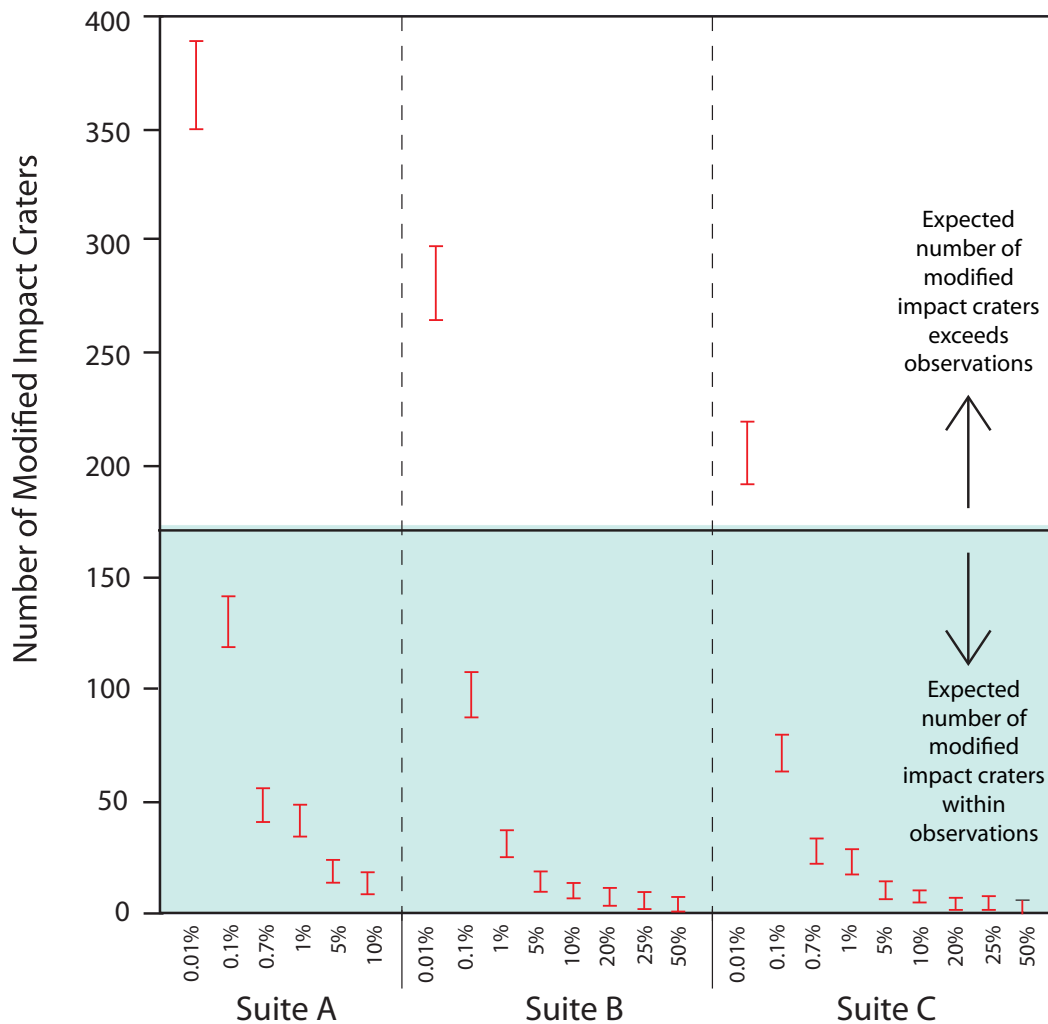
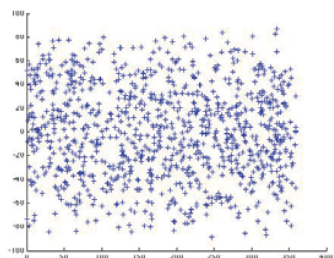
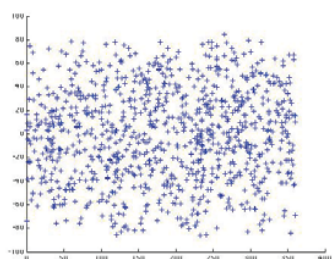


Figure 15: Graph showing which resulting impact crater distributions reproduce the low number of modified impact craters observed on Venus. The error bars represent one standard deviation from the mean in each experiment. The blue area at the bottom represents acceptable numbers of modified impact craters observed on a simulated planets surface.

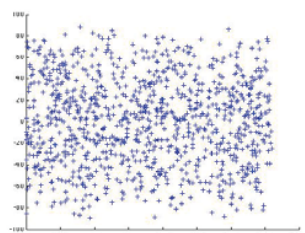
0.01% Resurfacing



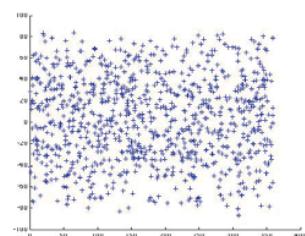
Test Run 188



Test Run 300

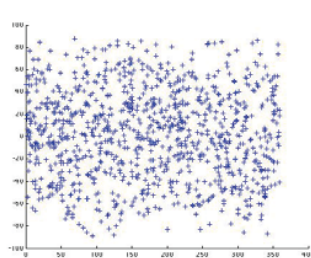


Test Run 521

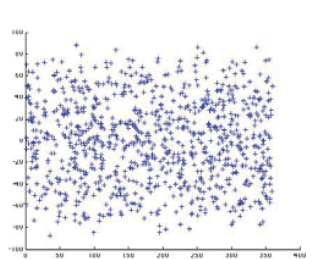


Test Run 684

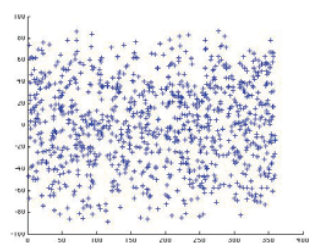
0.1% Resurfacing



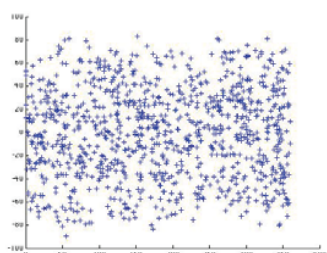
Test Run 8



Test Run 190

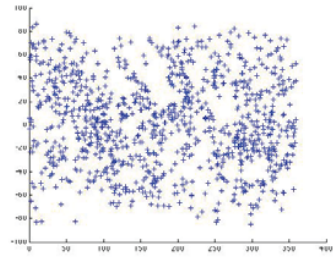


Test Run 261

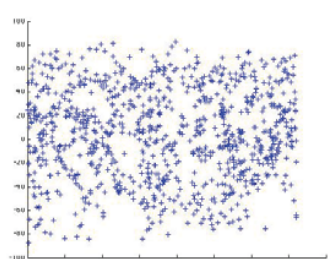


Test Run 569

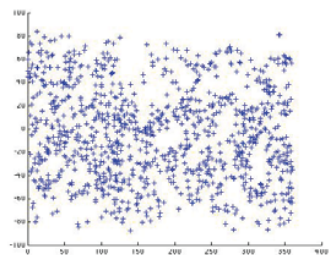
0.7% Resurfacing



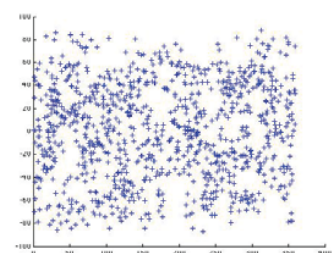
Test Run 348



Test Run 394



Test Run 600



Test Run 775

Figure 16A: Four sample surface impact crater distributions from 0.01%, 0.1%, and 0.7% resurfacing experiments in Suite A.

1% Resurfacing

5% Resurfacing

10% Resurfacing

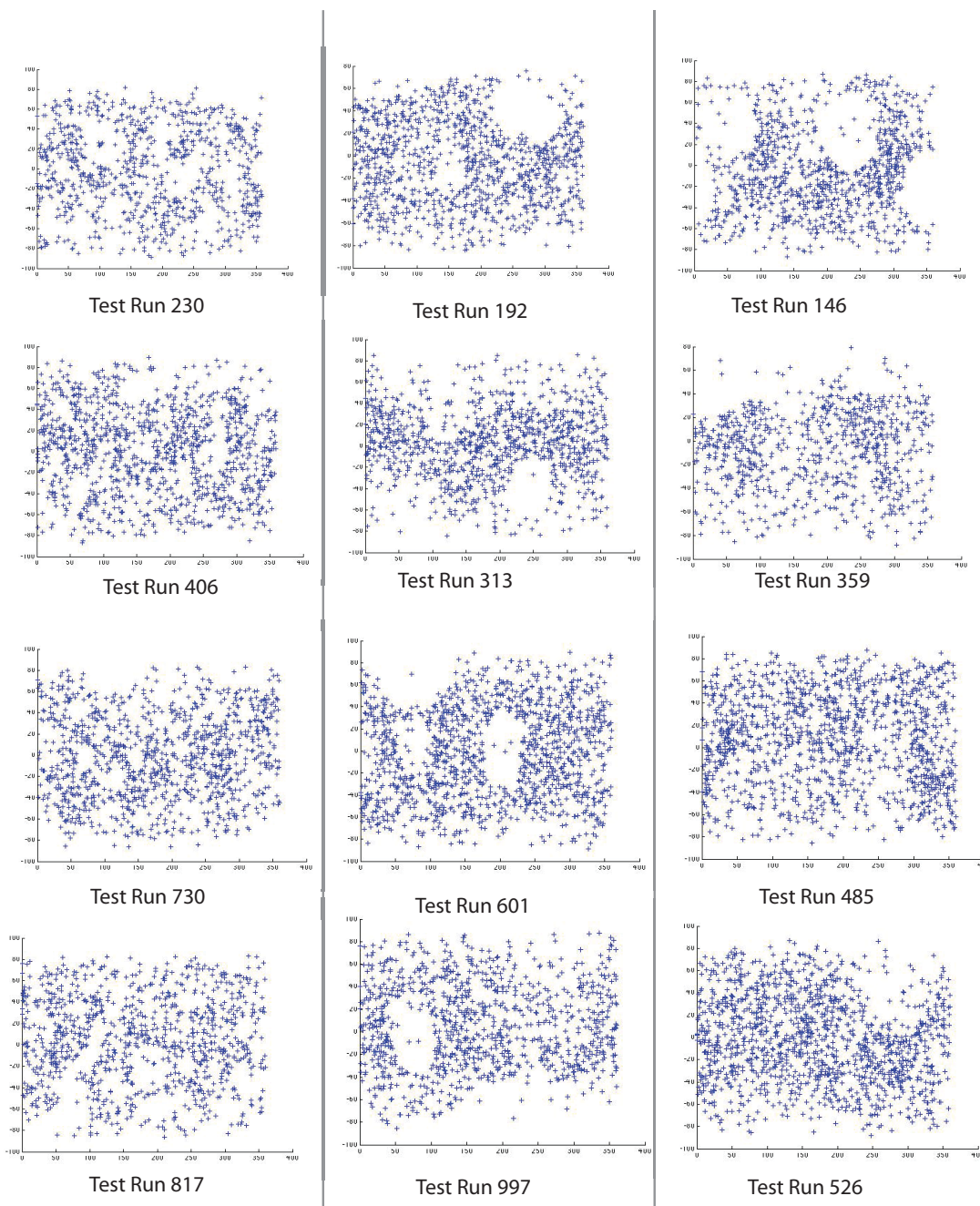
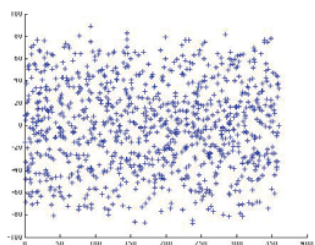
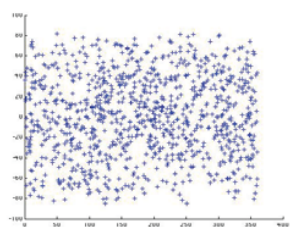


Figure 16B: Four sample surface impact crater distributions from 1%, 5%, and 10% resurfacing experiments in Suite A.

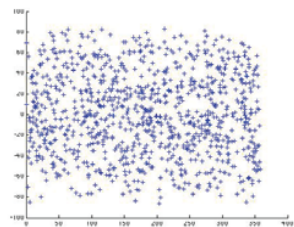
0.01% Resurfacing



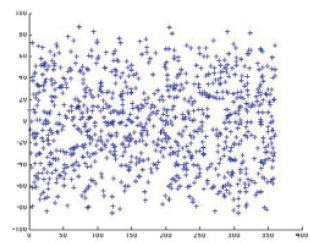
Test Run 122



Test Run 239

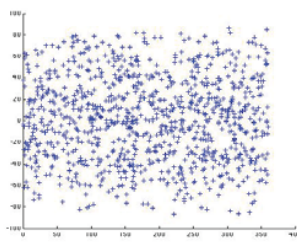


Test Run 576

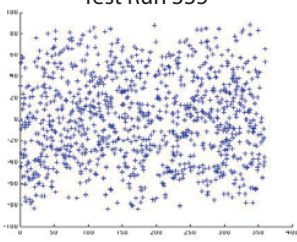


Test Run 855

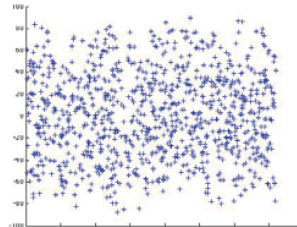
0.1% Resurfacing



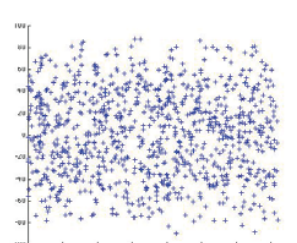
Test Run 335



Test Run 479

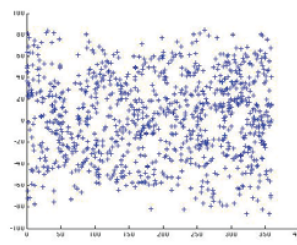


Test Run 714

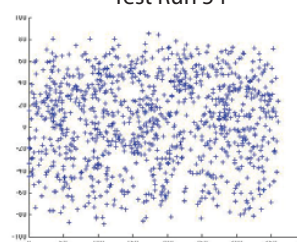


Test Run 985

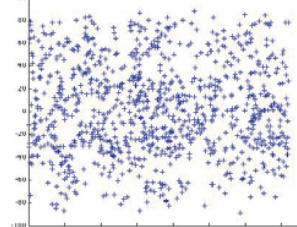
1% Resurfacing



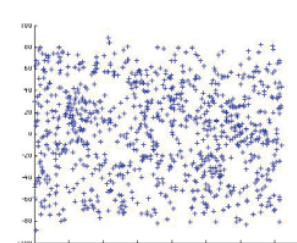
Test Run 54



Test Run 270



Test Run 486



Test Run 619

Figure 17A: Four sample surface impact crater distributions from 0.01%, 0.1%, and 1% resurfacing experiments in Suite B.

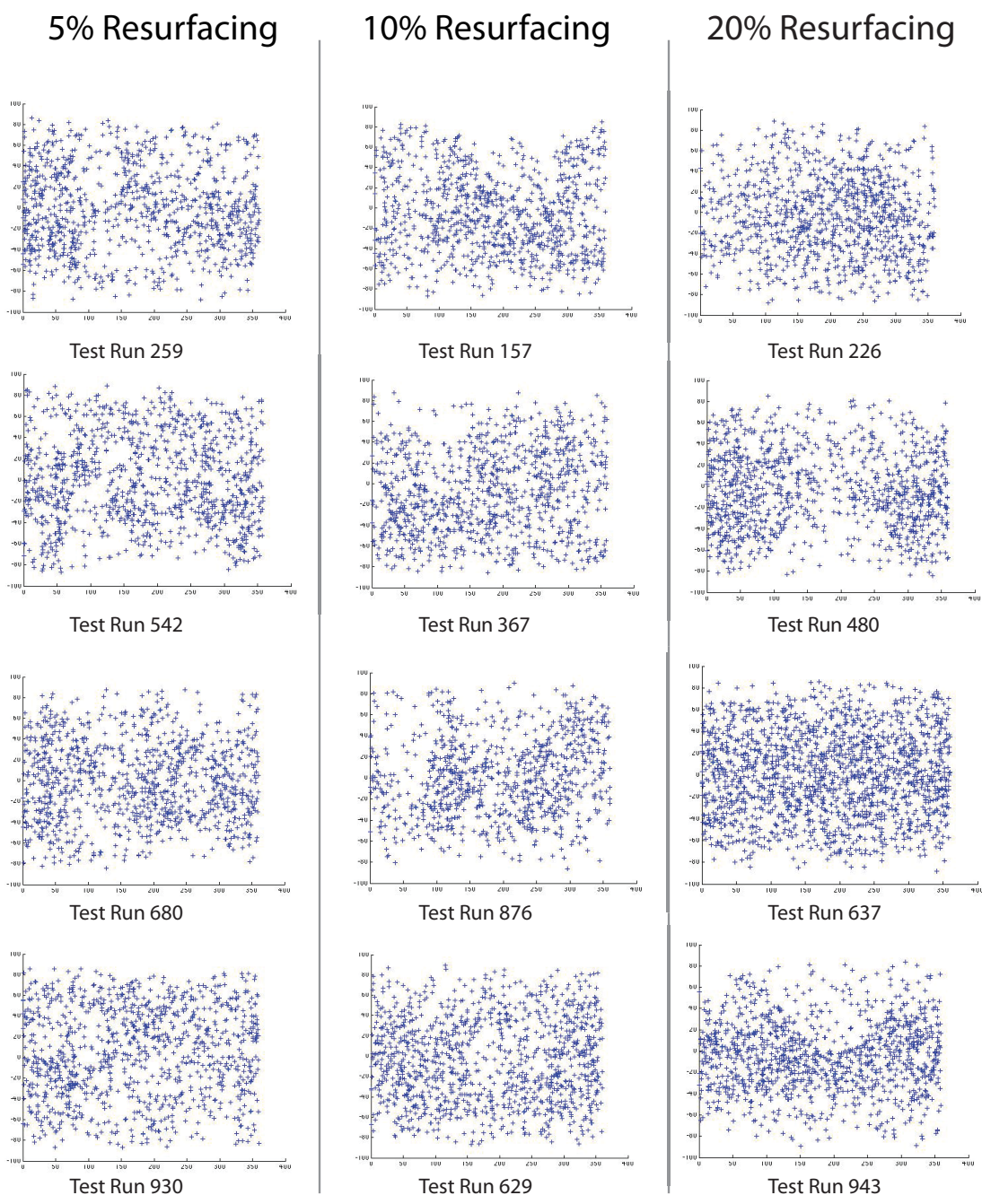
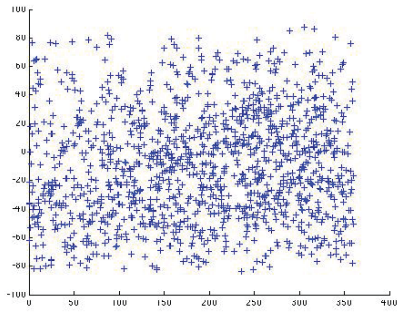
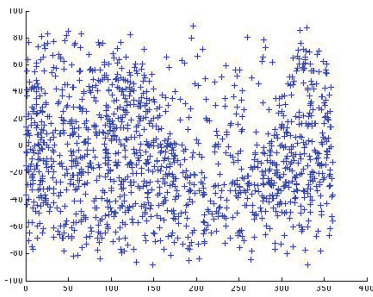


Figure 17B: Four sample surface impact crater distributions from 5%, 10%, and 20% resurfacing experiments in Suite B.

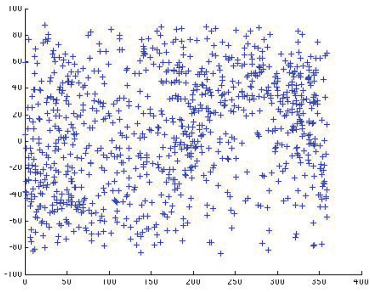
25% Resurfacing



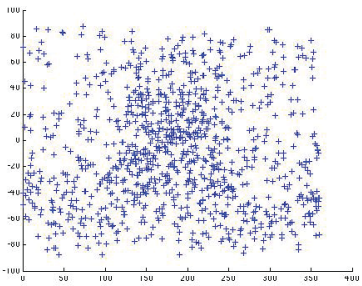
Test Run 169



Test Run 365

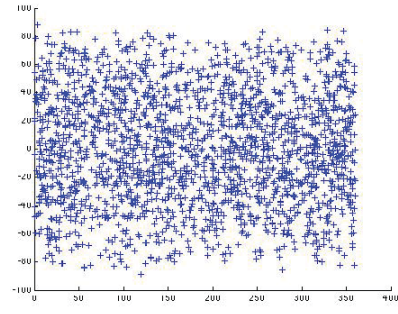


Test Run 810

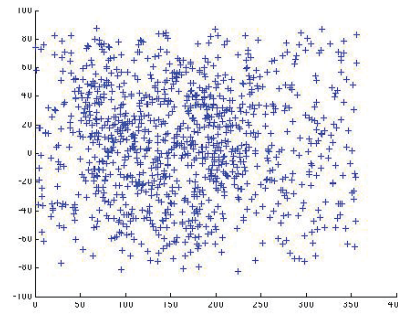


Test Run 998

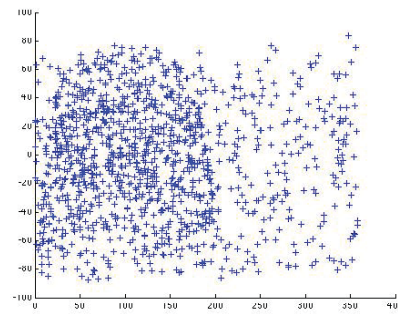
50% Resurfacing



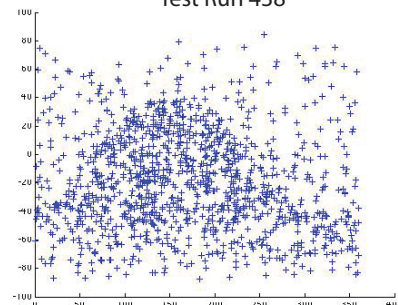
Test Run 2



Test Run 275



Test Run 438



Test Run 674

Figure 17C: Four sample surface impact crater distributions from 25% and 50% resurfacing experiments in Suite B.

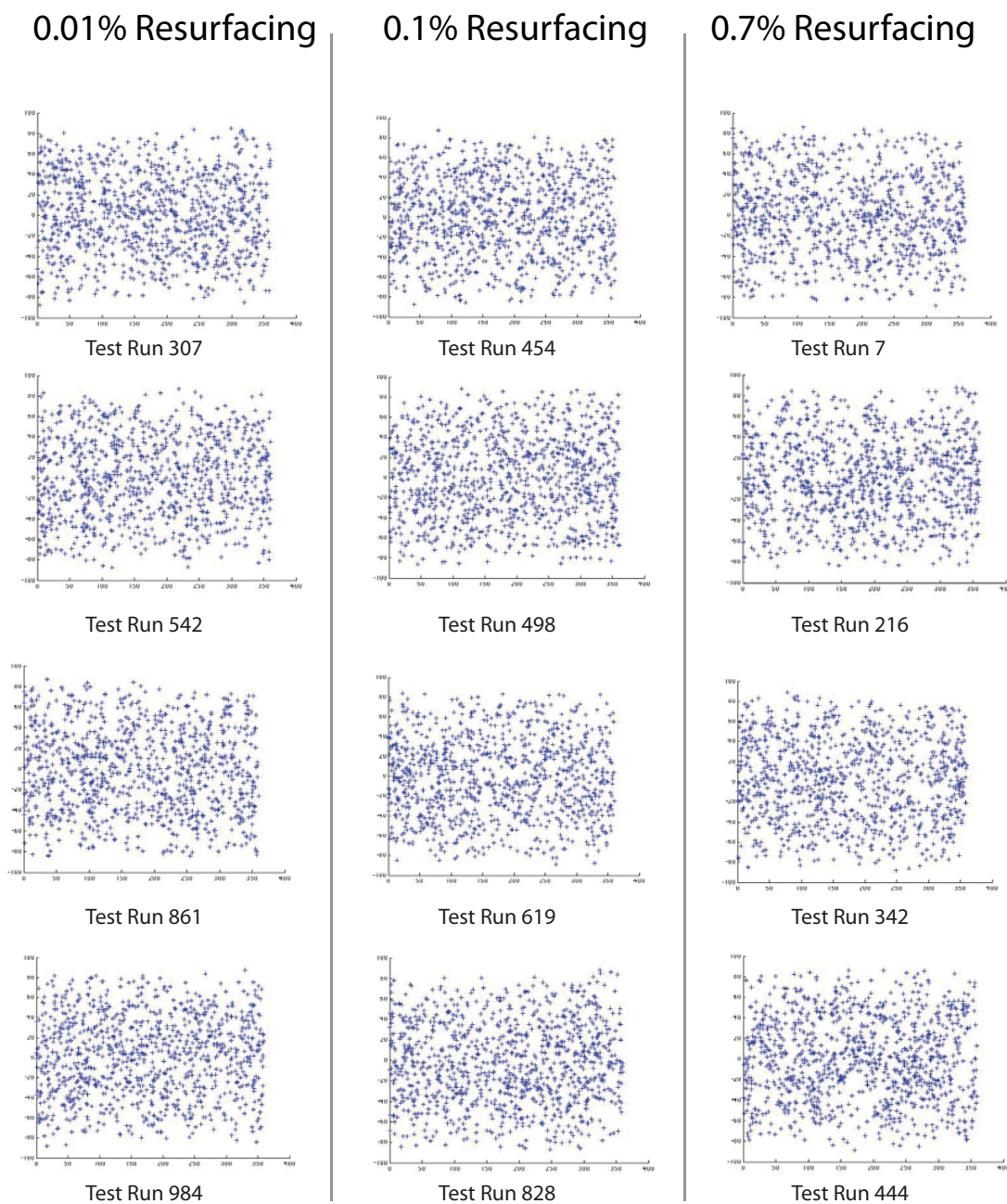
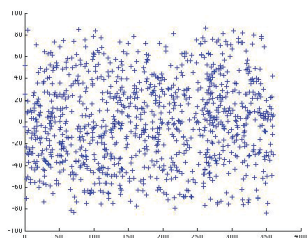
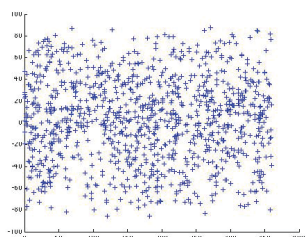


Figure 18A: Four sample surface impact crater distributions from 0.01%, 0.1%, and 0.7% resurfacing experiments in Suite C.

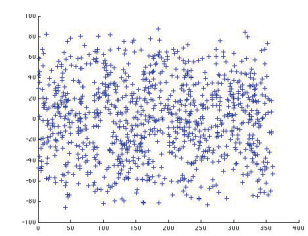
20% Resurfacing



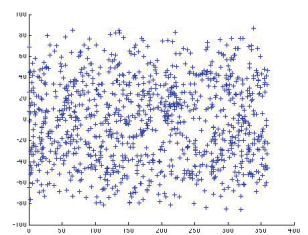
Test Run 367



Test Run 486

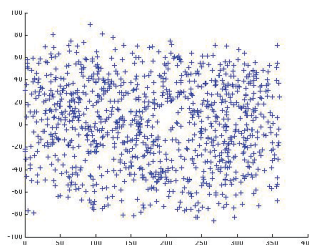


Test Run 601

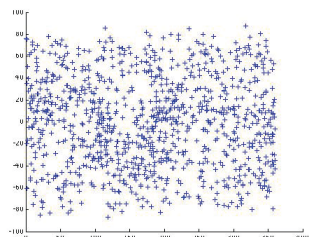


Test Run 954

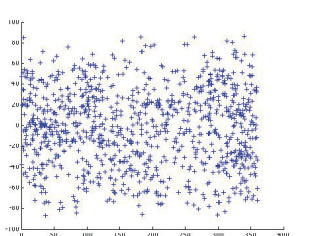
20% Resurfacing



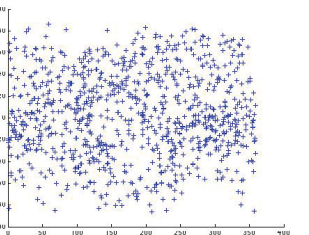
Test Run 118



Test Run 321

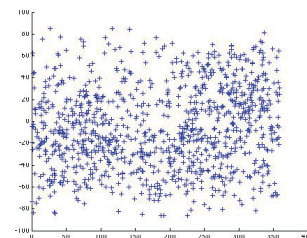


Test Run 476

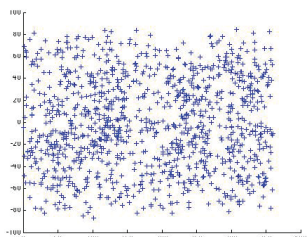


Test Run 718

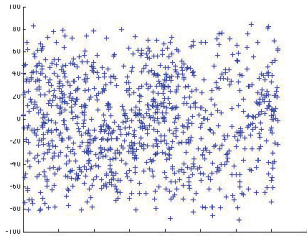
20% Resurfacing



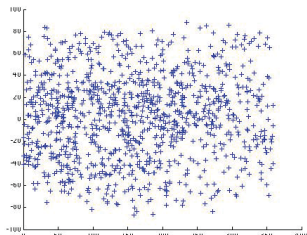
Test Run 7



Test Run 230



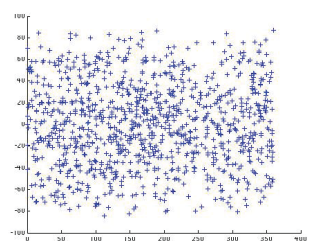
Test Run 575



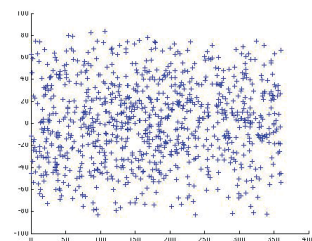
Test Run 692

Figure 18B: Four sample surface impact crater distributions from 1%, 5%, and 10% resurfacing experiments in Suite C.

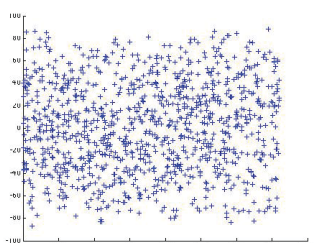
20% Resurfacing



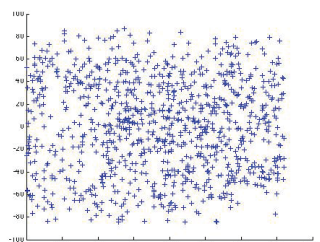
Test Run 42



Test Run 165

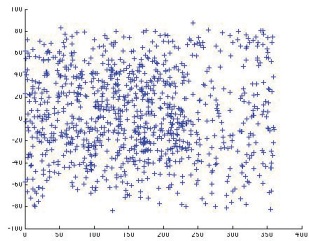


Test Run 380

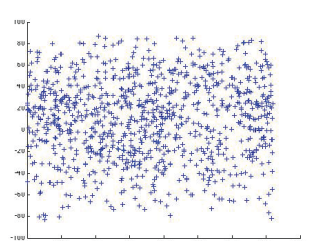


Test Run 760

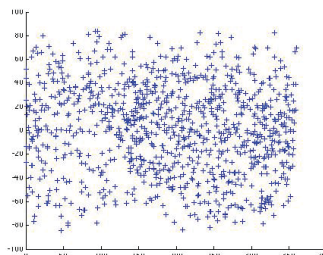
25% Resurfacing



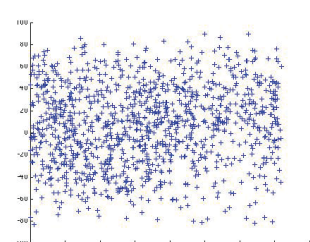
Test Run 132



Test Run 299

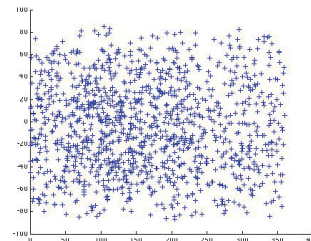


Test Run 707

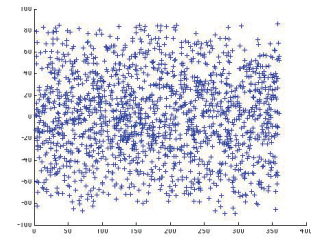


Test Run 944

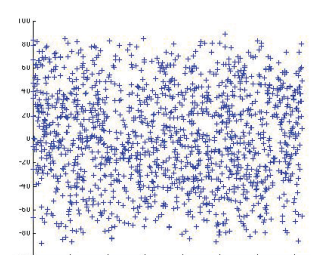
50% Resurfacing



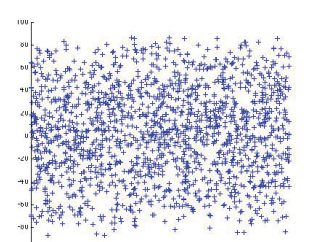
Test Run 252



Test Run 358



Test Run 592



Test Run 875

Figure 18C: Four sample surface impact crater distributions from 20%, 25%, and 50% resurfacing experiments in Suite C.

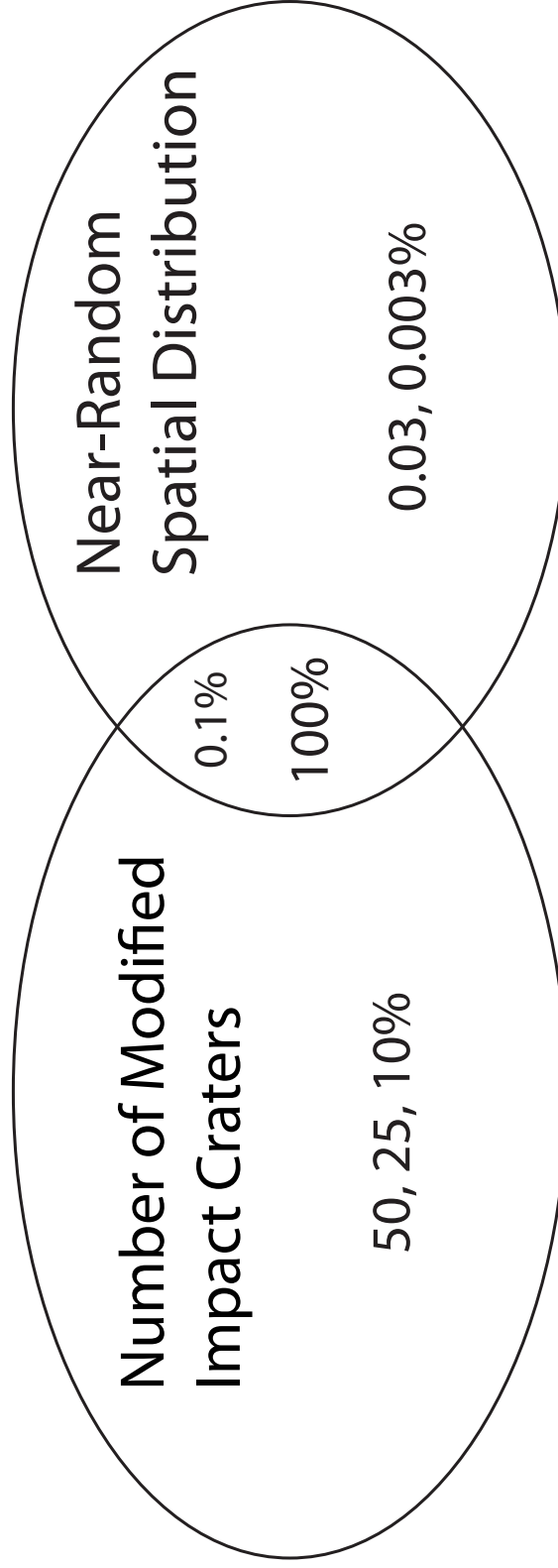


Figure 19: Venn diagram illustrating the resurfacing areas which were tested and which constraints they each meet under equilibrium resurfacing.

Number of Modification Events Per Impact Crater

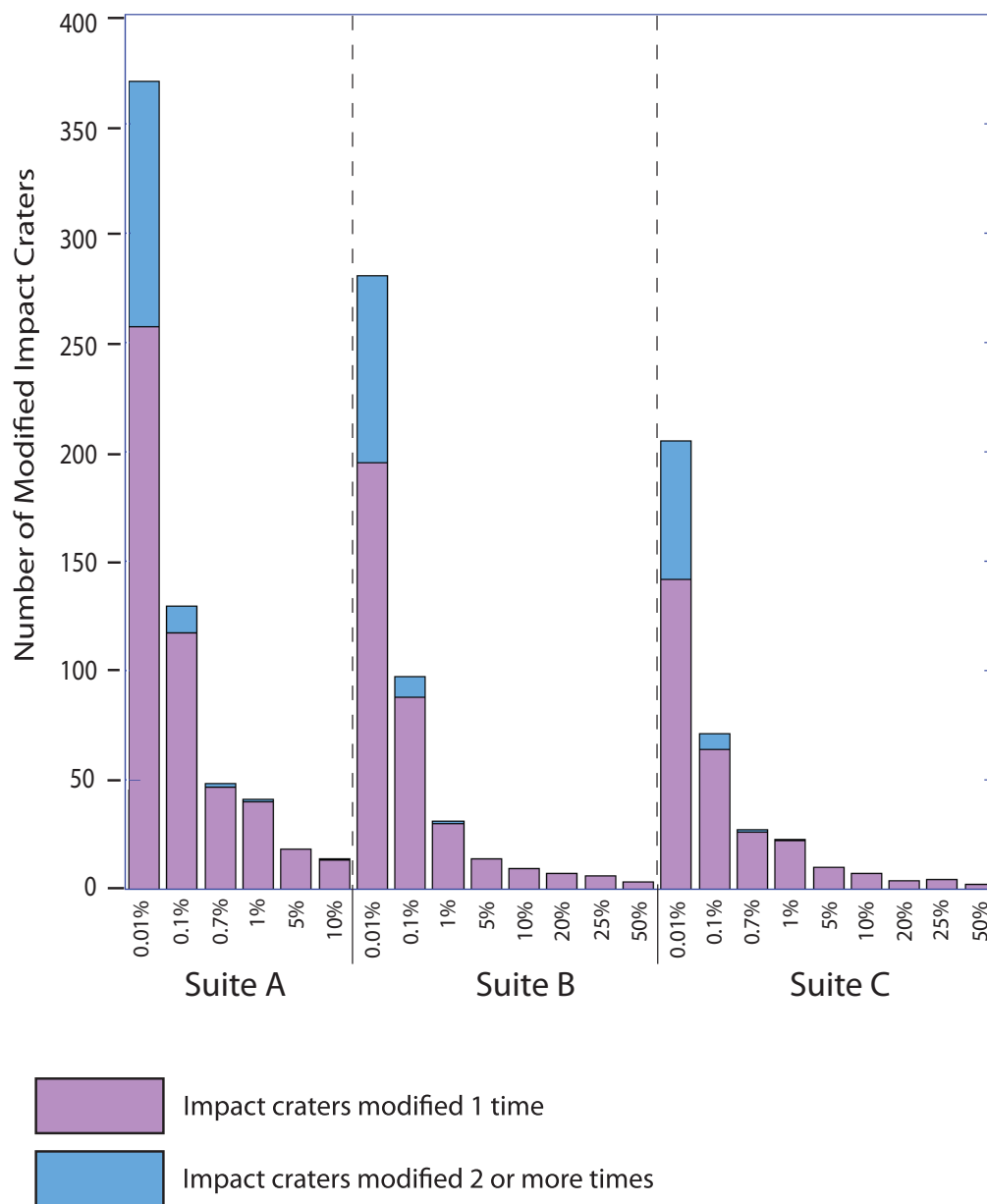


Figure 20: Graph illustrating the proportions of modified impact craters undergoing one modification event compared to those undergoing two or more events.

Appendix I: Geometric Series and the determination of time scales

The procedure for independently determining the impact crater formation and resurfacing time scales operates around the following assumptions:

- The final number of impact craters on the surface is 1000,
- Resurfacing events always have the same area,
- A time step is defined as the time in between resurfacing events, and
- The duration of impact crater formation is 4500 Ma (the entire duration of the test run).

Additionally, we will need the following definitions and relationships:

T_R is the duration of resurfacing event. Possible values are 4500, 3750, and 3000 Ma. This remains constant throughout a suite of experiments.

A_R is the size of the resurfaced area in the experiment. Possible values include 0.5, 0.25, 0.2, 0.1, 0.05, 0.01, 0.007, 0.001, and 0.0001. This remains constant throughout an experiment.

N_R is the number of expected resurfacing events in an experiment. Possible values are 2, 4, 5, 10, 100, 143, 1000, and 10000. This value is not held constant for all test runs in an experiment but rather serves as a Poisson mean about which the distribution of number of resurfacing events in an experiment is normally distributed.

$$N_R = 1/A_R$$

t_R is the length of time between resurfacing events.

$$t_R = T_R/N_R$$

T_C is the length of time during which only impact crater formation occurs.

$$T_C = 4500 - T_R$$

To calculate the number of impact craters emplaced in between resurfacing events, I set up a loop using the following parameters:

- n_i is the number of impact craters formed in one particular time step.
- $n_{t(x)}$ is the number of impact craters on the surface at the start of one particular time step.
- N_{Tx} is the number of impact craters on the surface at the end of one particular time step.

With these definitions, the following relationships hold:

$$\text{Total number of time steps} = N_R + N_I$$

If there are $n_{t(x)}$ impact craters on the surface at the start of a time step, and n_i impact craters added during the time step, and the resurfaced area in that test run is A_R , then there are

$$(n_i + n_{t(x)})(1 - A_R) = n_{t(x+1)}$$

impact craters on the surface at the start of the next test run. Another way of looking at this is through the following table, illustrating how the number of impact craters on the surface after each 25%-area resurfacing event changes with each time step:

$n_{t(x)}$	n_i	A_R	$1 - A_R$	# on surface before resurfacing event	$n_{t(x+1)}$
0	X	0.25	0.75	X	0.75X
0.75X	X	0.25	0.75	1.75X	1.3125X
1.3125X	X	0.25	0.75	2.3125X	1.7344
1.7344X	X	0.25	0.75	2.7344X	2.0508X

Even though a total of 4X impact craters were added to the surface throughout the test run, only 2.0508X impact craters remained there after the resurfacing events. I used MatLab to write a script using AR, TR, and TC to calculate the number of impact craters which form between each resurfacing event. As in the case above, the number of impact craters formed in each time step would be

$$X = 1000/2.0508 = 487.6146.$$

We can then find the length of time in between impact crater formation events through the formula

$$n_{\text{impact}} = n_R/n_i.$$

We now have all the information necessary to generate time scales for both impact crater formation and resurfacing. The final step is to generate exponentially-distributed random variables using Poisson means related to n_{impact} and n_R . The first generated random-variable for impact crater formation corresponds to the time needed to form the first impact crater, then the second generated random variable corresponds to the time needed for the second impact crater to form after the first one, etc. until the sum of the randomly generated variable sum up to larger than 4500. This is because 4500 is the duration of the test run. Follow the same procedure to generate the time scale for the resurfacing events.

Appendix II: Sample MatLab Script for Test Runs

```

% MATLAB file to run better STROM Tests
% Finished 6/27/07 by Emily Bjonnes

T = 4500;
n = input('Enter the number of times to run the experiment: ');
ct = input('Enter the average time between craters: '); % define
the time between craters
pt = input('Enter the average time between plateaus: '); % define
the time between plateaus
Dc = input('Enter the average diameter of an impact crater (km): ');
% define the average size of an impact crater
Rcp = input('Enter the average radius of a crustal plateau (km): ');
%define the average size of a plateau
Rv = 6052; % define the size of Venus

for i=1:n
    filename = sprintf('stromcraters_test9_%d.mat',i);

    U = rand(1,1);
    PT = -pt*log(U);
    Plat_Time = [PT];
    Total_Platt_Time = sum(Plat_Time);
    Cum_Platt_Time = [Total_Platt_Time];

    while Total_Platt_Time < T
        U = rand(1,1);
        PT = -pt*log(U);
        Plat_Time = [Plat_Time; PT];
        Total_Platt_Time = sum(Plat_Time);
        Cum_Platt_Time = [Cum_Platt_Time; Total_Platt_Time];
    end

    L = length(Cum_Platt_Time);

    N = L-1;

    Plat_Time(L) = [];

    Cum_Platt_Time(L) = [];

    V = rand(1,1);
    CT = -ct*log(V);
    Crat_Time = [CT];
    Total_Crat_Time = sum(Crat_Time);
    Cum_Crat_Time = [Total_Crat_Time];

    while Total_Crat_Time < T
        V = rand(1,1);
        CT = -ct*log(V);
        Crat_Time = [Crat_Time; CT];
        Total_Crat_Time = sum(Crat_Time);
    end
end

```

```

    Cum_Crat_Time = [Cum_Crat_Time; Total_Crat_Time];
end

M = length(Cum_Crat_Time);

Crat_Time(M) = [];

Cum_Crat_Time(M) = [];

a = find(Cum_Crat_Time <= Cum_Plat_Time(1,1));
b = length(a);
A = [b];

for ij = 2:N
    ii = ij-1;
    P_Up = Cum_Plat_Time(ij,1);
    P_Down = Cum_Plat_Time(ii,1);

    a = find(Cum_Crat_Time <= P_Up & Cum_Crat_Time > P_Down);
    b = length(a);
    A = [A; b];
end

f = find(Cum_Crat_Time > Cum_Plat_Time(N));
F = length(f);

clear U PT V CT a b ij ii P_Up P_Down

cxr = [];
cyr = [];
czr = [];
cer = [];

cxe = [];
cye = [];
cze = [];
cee = [];

inner_radius = (Rcp-Dc)/Rv*180/3.1415; % define the inner radius
for edge effects
outer_radius = (Rcp+Dc)/Rv*180/3.1415; % define the outer radius
for edge effects

Time = [];
Plateaus = [];
Num_Craters_Saved = [];
Num_Craters_Destroyed = [];
Num_Craters_Edge = [];
Destroyed_Craters = [];
Edge_Craters = [];

for ij = 1:N

```

```

CT = A(ij);

if CT == 0
    cx = [cxr cxe];
    cy = [cyr cye];
    cz = [czt cze];
    ce = [cer cee];

    crater = [cx' cy' cz' ce']; % combine craters coordinates
for old and new craters
    Total_Craters = length(cx); %find the number of craters
you need to consider in this time step

    pxn = rand(1,1)*2-1;
    pyn = rand(1,1)*2-1;
    pzn = rand(1,1)*2-1;
    p_distance = pxn^2 + pyn^2 + pzn^2;
while p_distance > 1
    pxn = rand(1,1)*2-1;
    pyn = rand(1,1)*2-1;
    pzn = rand(1,1)*2-1;
    p_distance = pxn^2 + pyn^2 + pzn^2;
end

% ---- Normalize the Radius -----

px = pxn / p_distance^(1/2);
py = pyn / p_distance^(1/2);
pz = pzn / p_distance^(1/2);

% ----- Put it in a Matrix -----

Plateau = [px py pz];

if Total_Craters == 0

    Time = [Time; ij];

    Plateaus = [Plateaus; Plateau];

    Num_Craters_Saved = [Num_Craters_Saved; 0];
    Num_Craters_Destroyed = [Num_Craters_Destroyed; 0];
    Num_Craters_Edge = [Num_Craters_Edge; 0];
    Destroyed_Craters = [Destroyed_Craters];
    Edge_Craters = [Edge_Craters];

else
    plateaus = zeros(Total_Craters,4);
    plateaus(:,1) = px; plateaus(:,2) = py; plateaus(:,3) =
pz; plateaus(:,4) = 0; % generate plateau coordinates into a matrix
    plateaus;

    dot_terms = plateaus.*crater;

```



```

Saved_Craters = length(cxr);

Craters_Destroyed = [cxd' cyd' czd' ced'];
D = length(cxd);

Craters_Edge = [cxe' cye' cze' cee'];
Edge = length(cxe);

Final_Num_Saved = Saved_Craters+Edge;

Num_Craters_Saved = [Num_Craters_Saved;
Final_Num_Saved];
Num_Craters_Destroyed = [Num_Craters_Destroyed; D];
Num_Craters_Edge = [Num_Craters_Edge; Edge];
Destroyed_Craters = [Destroyed_Craters;
Craters_Destroyed];
Edge_Craters = [Edge_Craters; Craters_Edge];
end

else
    cxn = rand(1,1)*2-1;    % create x values for new crater
locations
    cyn = rand(1,1)*2-1;    % create y values for new crater
locations
    czn = rand(1,1)*2-1;

    craters_new = [cxn cyn czn];
    craters_new = craters_new.^2;
    craters = [];
    craters = (craters_new(:,1) + craters_new(:,2) +
craters_new(:,3));
    craters = craters.^(1/2);

    inside = find(craters <= 1);
    in = length(inside);
    outside = find(craters > 1);
    out = length(outside);

    cxn = cxn(inside);
    cyn = cyn(inside);
    czn = czn(inside);

    % ---- Make Sure you Generate Enough Craters -----

    while in<CT
        cxn_more = rand(1,1)*2 - 1;    % generate more x-
coords of crater centers
        cyn_more = rand(1,1)*2 - 1;    % generate more y-
coords of crater centers
        czn_more = rand(1,1)*2 - 1;    %generate more z-coords
of crater centers

        cxnew = [cxn cxn_more];

```

```

    cynew = [cyn cyn_more];
    cznew = [czn czn_more];

    total_craters = [cxnew' cynew' cznew'];
    total_craters = total_craters.^2;
    craters = [];
    craters = (total_craters(:,1) + total_craters(:,2) +
total_craters(:,3));
    craters = craters.^(1/2);

    inside = find(craters <= 1);
    in = length(inside);
    outside = find(craters > 1);
    out = length(outside);

    cxn = cxnew(inside);
    cyn = cynew(inside);
    czn = cznew(inside);
end

    dist = craters(inside);
    dist_inverse = dist.^(-1);
    inverse_crater_distances = [dist_inverse dist_inverse
dist_inverse];

    craters_inside = [cxn' cyn' czn'];
    new_craters = craters_inside.*inverse_crater_distances;

    cxn = new_craters(:,1);
    cyn = new_craters(:,2);
    czn = new_craters(:,3);
    cen = zeros(in,1);

    cx = [cxn' cxr cxe];
    cy = [cyn' cyr cye];
    cz = [czn' czr cze];
    ce = [cen' cer cee];

    crater = [cx' cy' cz' ce']; % combine craters coordinates
for old and new craters
    Total_Craters = length(cx); %find the number of craters
you need to consider in this time step

    % --- Work With the Plateaus -----

    % ----- Generate Plateau Within Sphere-----

    pxn = rand(1,1)*2-1;
    pyn = rand(1,1)*2-1;
    pzn = rand(1,1)*2-1;
    p_distance = pxn^2 + pyn^2 + pzn^2;
    while p_distance > 1
        pxn = rand(1,1)*2-1;

```



```

    cee = ce(edge);
    cee = cee + 1;
    cee = reshape(cee,1,R);

    cxd = cx(destroyed);    % find x coords for destroyed
craters
    R = length(cxd);
    cxd = reshape(cxd,1,R); % reshape it into a row vector
    cyd = cy(destroyed);    % find y coords for destroyed
craters
    cyd = reshape(cyd,1,R); % reshape it into a row vector
    czd = cz(destroyed);    % find z coords of destroyed
craters
    czd = reshape(czd,1,R); % reshape it into a row vector
    ced = ce(destroyed);
    ced = reshape(ced,1,R);

    Time = [Time; ij];

    Plateaus = [Plateaus; Plateau];

    Craters_Remaining = [cxr' cyr' czr' cer'];
    Saved_Craters = length(cxr);

    Craters_Destroyed = [cxd' cyd' czd' ced'];
    D = length(cxd);

    Craters_Edge = [cxe' cye' cze' cee'];
    Edge = length(cxe);

    Final_Num_Saved = Saved_Craters+Edge;

    Num_Craters_Saved = [Num_Craters_Saved; Final_Num_Saved];
    Num_Craters_Destroyed = [Num_Craters_Destroyed; D];
    Num_Craters_Edge = [Num_Craters_Edge; Edge];
    Destroyed_Craters = [Destroyed_Craters; Craters_Destroyed];
    Edge_Craters = [Edge_Craters; Craters_Edge];

end

end

if F == 0
    Time = [Time];
    Num_Craters_Saved = [Num_Craters_Saved];
    Num_Craters_Destroyed = [Num_Craters_Destroyed];
    Num_Craters_Edge = [Num_Craters_Edge];
    Destroyed_Craters = [Destroyed_Craters];
    Edge_Craters = [Edge_Craters];

    cx = [cxr cxe];
    cy = [cyr cye];
    cz = [cyr cze];

```

```

ce = [cer cee];

else
    CT = F;
    cxn = rand(1,1)*2-1;    % create x values for new crater
locations
    cyn = rand(1,1)*2-1;    % create y values for new crater
locations
    czn = rand(1,1)*2-1;

    craters_new = [cxn cyn czn];
    craters_new = craters_new.^2;
    craters = [];
    craters = (craters_new(:,1) + craters_new(:,2) +
craters_new(:,3));
    craters = craters.^(1/2);

    inside = find(craters <= 1);
    in = length(inside);
    outside = find(craters > 1);
    out = length(outside);

    cxn = cxn(inside);
    cyn = cyn(inside);
    czn = czn(inside);

    % ---- Make Sure you Generate Enough Craters -----

    while in<CT
        cxn_more = rand(1,1)*2 - 1;    % generate more x-coords of
crater centers
        cyn_more = rand(1,1)*2 - 1;    % generate more y- coords of
crater centers
        czn_more = rand(1,1)*2 - 1;    %generate more z-coords of
crater centers

        cxnew = [cxn cxn_more];
        cynew = [cyn cyn_more];
        cznew = [czn czn_more];

        total_craters = [cxnew' cynew' cznew'];
        total_craters = total_craters.^2;
        craters = [];
        craters = (total_craters(:,1) + total_craters(:,2) +
total_craters(:,3));
        craters = craters.^(1/2);

        inside = find(craters <= 1);
        in = length(inside);
        outside = find(craters > 1);
        out = length(outside);

        cxn = cxnew(inside);

```

```

        cyn = cynew(inside);
        czn = cznew(inside);
    end

    dist = craters(inside);
    dist_inverse = dist.^(-1);
    inverse_crater_distances = [dist_inverse dist_inverse
dist_inverse];

    craters_inside = [cxn' cyn' czn'];
    new_craters = craters_inside.*inverse_crater_distances;

    cxn = new_craters(:,1);
    cyn = new_craters(:,2);
    czn = new_craters(:,3);
    cen = zeros(in,1);

    cx = [cxn' cxr cxe];
    cy = [cyn' cyr cye];
    cz = [czn' czr cze];
    ce = [cen' cer ceel];

    ij = Time(N)+1;
    Time = [Time; ij];

    A = [A; F];

    Num_Craters_Saved = [Num_Craters_Saved; F];
    Num_Craters_Destroyed = [Num_Craters_Destroyed; 0];
    Num_Craters_Edge = [Num_Craters_Edge; 0];
    Destroyed_Craters = [Destroyed_Craters];
    Edge_Craters = [Edge_Craters];

end

Remaining_Craters = [cx' cy' cz' ce'];

clear C F CT ij Craters_Destroyed Craters_Edge Craters_Remaining D
Edge Final_Num_Saved L M N Plateau R Saved_Craters Total_Crat_Time
Total_Craters Total_Plat_Time ans ce ced cee cer cen crater craters
craters_inside craters_new cx cxd cxe cxn cxr cxn_more cxnew cy cyd cye
cyn cyn_more cynew cyr cz czd cze czn czn_more cznew czr deg destroyed
dist dist_inverse dot_terms edge f i in inner_radius inside
inverse_crater_distances new_craters out outer_radius outside
p_distance plateaus px py pz pyn pxn pzn remain s total_craters

B = Remaining_Craters;

Bx = B(:,1);
By = B(:,2);
Bz = B(:,3);

Bx2 = Bx*Bx';

```

```

By2 = By*By';
Bz2 = Bz*Bz';

dist = Bx2 + By2 +Bz2;

dist = acos(dist);

r = length(Bx);

D = [];

for ii = 1:(r-1)
    K = diag(dist,ii);
    D = [D; K];
end

clear Bx2 By2 Bz2 ii

cx = Remaining_Craters(:,1);
cy = Remaining_Craters(:,2);
cz = Remaining_Craters(:,3);
cer = Remaining_Craters(:,4);
ced = Destroyed_Craters(:,4);
ce = [cer; ced];

a = find(cx >=0 & cy >=0);
b = find(cx < 0 & cy >= 0);
c = find(cx < 0 & cy < 0);
d = find(cx >= 0 & cy < 0);

cx1 = cx(a);
cy1 = cy(a);
cz1 = cz(a);

cx2 = cx(b);
cy2 = cy(b);
cz2 = cz(b);

cx3 = cx(c);
cy3 = cy(c);
cz3 = cz(c);

cx4 = cx(d);
cy4 = cy(d);
cz4 = cz(d);

lon1 = atan(cy1./cx1).*180/pi;
lat1 = asin(cz1).*180/pi;

lon2 = atan(cy2./cx2).*180/pi+180;
lat2 = asin(cz2).*180/pi;

```

```

lon3 = atan(cy3./cx3).*180/pi+180;
lat3 = asin(cz3).*180/pi;

lon4 = atan(cy4./cx4).*180/pi+360;
lat4 = asin(cz4).*180/pi;

lon = [lon1; lon2; lon3; lon4];
lat = [lat1; lat2; lat3; lat4];

craters_globe = [lon lat];

avg_saved_per_time_step = mean(Num_Craters_Saved);

avg_destroyed_per_time_step = mean(Num_Craters_Destroyed);

avg_edge_per_time_step = mean(Num_Craters_Edge);

Total_Num_Edge_Effects = sum(ce);

a = find(D <= 0.05);
b = length(a);
cum_dist = [b];
binned = [b];

for ii = 2:63
    n = 0.05*ii;
    a = find(D <= n);
    b = length(a);
    c = ii-1;
    e = cum_dist(c);
    f = b-e;
    cum_dist = [cum_dist; b];
    binned = [binned; f];
end

K = length(Num_Craters_Saved);
B = zeros(K,1);
B(:,1) = avg_saved_per_time_step;
S2 = Num_Craters_Saved - B;
S2 = S2.^2;
total = sum(S2);
S2 = total/K;
Sigma_Saved = S2.^0.5;

clear B K S2 total ii

K = length(Num_Craters_Edge);
B = zeros(K,1);
B(:,1) = avg_edge_per_time_step;

```

```

S2 = Num_Craters_Edge - B;
S2 = S2.^2;
total = sum(S2);
S2 = total/K;
Sigma_Edge = S2.^0.5;

clear K B S2 total

M = max(binned);
B = length(binned);
x = 0.025:0.05:3.125;
X = x';
F = M*sin(X);
S2 = binned - F;
S2 = S2.^2;
total = sum(S2);
S2 = total/B;
Sigma_Dist = S2.^0.5;

clear ans

save(filename, 'binned', 'cum_dist', 'A', 'Edge_Craters', 'Sigma_Edge', 'Sigma_Saved', 'Sigma_Dist', 'craters_globe', 'D', 'avg_saved_per_time_step', 'avg_destroyed_per_time_step', 'avg_edge_per_time_step', 'Total_Num_Edge_Effects', 'T', 'Dc', 'Rcp', 'Rv', 'pt', 'ct', 'Time', 'Plateaus', 'Remaining_Craters', 'Time', 'Num_Craters_Saved', 'Num_Craters_Destroyed', 'Num_Craters_Edge', 'Destroyed_Craters', 'A', 'Crat_Time', 'Cum_Crat_Time', 'Cum_Plat_Time')

clear Bx By Bz Total Crat_Time Cum_Crat_Time Cum_Plat_Time
Destroyed_Craters Edge_Craters Num_Craters_Destroyed Num_Craters_Edge
Num_Craters_Saved Plat_Time Plateaus Remaining_Craters Time
craters_globe Contine Num_Craters_Added M B x X F S2 total lat lon
Num_Craters_Added Sigma_Dist Sigma_Edge Sigma_Saved a b cum_dist binned
ii n c e f A Ax Ay Az dist r ii B D cx cy cz cer ced ce a b c d cx1 cx2
cx3 cx4 cy1 cy2 cy3 cy4 cz1 cz2 cz3 cz4 lon1 lon2 lon3 lon4 lat1 lat2
lat3 lat4 avg_saved_per_time_step avg_destroyed_per_time_step
avg_edge_per_time_step Total_Num_Edge_Effects

i

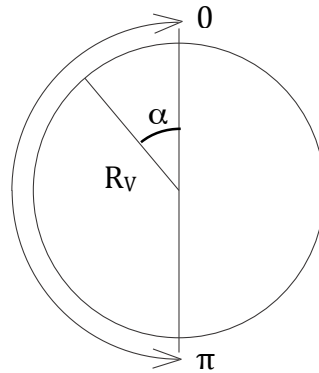
end

```

Appendix III: Finding the line of best fit around a histogram of intercrater distances

For any two impact craters, the possible angles defining the intercrater distance (α) must be between 0 and π (Figure 21):

Figure 21:



To create a frequency histogram for the distances between every set of impact craters, I calculated all intercrater angles in each test distribution and then binned them to create a frequency histogram. I extended the x-axis to a value of 3.15, slightly higher than the actual value of π , to make binning the values easier. The intercrater angles were binned in values of 0.05 radians, resulting in 63 final bins.

The general shape of the frequency histogram matches that of a sine curve because the majority of impact craters will lie nearest an angle of $\pi/2$ radians from a given impact crater. Consequently I will be fitting the frequency histogram to a sine curve. There is no preset formula for this, so the first step to finding the best-fit sine curve involves finding the area contained within the histogram. Each bin has a width of 0.05, and the height is the y-value, or frequency, of that range of angles. Adding the areas of each individual bin gives the total area within the histogram.

The next step is to integrate a generic sine curve and fit it to the histogram. The general form of the best fit line will be

$$f(\alpha) = M\sin(\alpha),$$

where α is again the intercrater angle and M is a scaling factor. Then we find that

$$F(\alpha) = \int_0^{\pi} M \sin(\alpha) d\alpha = M \int_0^{\pi} \sin(\alpha) d\alpha = -M[\cos(\pi) - \cos(0)].$$

$\cos(\pi)$ is equal to -1, and $\cos(0)$ is equal to 1, so $F(\alpha)$ equals $2M$.

One way to approximate the best fit line in this case is to set the two calculated areas equal and solve for the scaling factor in the sine curve (M). This equation is simply

$$2M=A_{\text{Hist}} \rightarrow M=A_{\text{Hist}}/2.$$

Finally, this value of M serves as the scaling factor in the sine curve, providing the equation for the best fit line as

$$f(\alpha)=A_{\text{Hist}}/2*\sin(\alpha)$$

REFERENCES

- Andersson, L.E., and Whitaker, E.A., 1982, NASA Catalogue of Lunar Nomenclature, NASA RP-1097.
- Banerdt, W. B., McGill, G. E., and Zuber, M. .T., 1997, Plains tectonics on Venus *in* Bougher, S.W., Hunten, D.M., and Phillips, R.J., eds., Venus II: Geology, Geophysics, Atmosphere, and Solar Wind Environment: Tucson, AZ, The University of Arizona Press, p. 901-930.
- Basilevsky, A.T., Head, J.W., and Setyaeva, I.V., 2003, Venus: Estimation of age of impact craters on the basis of degree of preservation of associated radar-dark deposits: Geophysical Research Letters, v. 30, p. 1950-1953.
- Basilevsky, A. T., Head, J. W., Schaber, G. G., and Strom, R. G., 1997, The resurfacing history of Venus, *in* Bougher, S.W., Hunten, D.M., and Phillips, R.J., eds., Venus II: Geology, Geophysics, Atmosphere, and Solar Wind Environment: Tucson, AZ, The University of Arizona Press, p. 1047-1086.
- Basilevsky, A. T., and Head, J. W., 1996, Evidence for rapid and widespread emplacement of volcanic plains on Venus: Stratigraphic studies in the Baltis Vallis region, Geophysical Research Letters, v. 23, p. 1497-1500.
- Basilevsky, A. T., and Head, J. W., 1995, Regional and global stratigraphy of Venus: a preliminary assessment and implications for the geological history of Venus, Planetary and Space Science, v. 43, no. 12, p. 1523-1553.
- Bindschadler, D. L., 1995, Magellan: A new view of Venus' geology and geophysics, Reviews of Geophysics, v. 33 no. S1, p. 459-468.
- Bindschadler, D.L., Schubert, G., and Kaula, W.M., 1992, Coldspots and hotspots: Global tectonics and mantle dynamic of Venus: Journal of Geophysical Research, v. 97, p. 13495-13532.
- Bindschadler, D.L., and Paramentier, E.M., 1990, Mantle flow tectonics: The influence of a ductile lower crust and implications for the formation of topographic uplands on Venus: Journal of Geophysical Research, v. 95, p. 21329-21344.
- Campbell, B.A., 1999, Surface formation rates and impact crater densities on Venus, Journal of Geophysical Research, v. 104, no. 21, p. 951-21,956.
- Crumpler, L. S., Aubele, J. C., Senske, D. A., Keddie, S. T., Magee, K. P. and Head, J. W., 1997, Volcanoes and centers of volcanism on Venus, *in* Bougher, S.W., Hunten, D.M., and Phillips, R.J., eds., Venus II: Geology, Geophysics, Atmosphere, and Solar Wind Environment: Tucson, AZ, The University of Arizona Press, p. 697.
- Culler., T. S., Becker, T. A., Muller., R. A., Renne, P. R., 2000, Lunar impact history from $^{40}\text{Ar}/^{39}\text{Ar}$ dating of glass spherules, Science, v. 287, no. 5459, p. 1785-1788.
- Earth Impact Database, 2007, Earth Impact Database, The Planetary and Space Centre, University of New Brunswick.
- Esposito, L.W., Bertaux, J.-L., Krasnopolsky, V., Moroz, V.I., and Zasova, L.V., 1997, Chemistry of the lower atmosphere and clouds, *in* Bougher, S.W., Hunten, D.M., and Phillips, R.J., eds., Venus II: Geology, Geophysics, Atmosphere, and Solar Wind Environment: Tucson, AZ, The University of Arizona Press, p. 415-458.

- Ford, J.P., Plaut, J.J., Weitz, C.M., Farr, T.G., Senske, D.A., Stofan, E.R., Micheals, G.A., and Parker, T.J., 1993, Guide to Magellan Image Interpretation: Pasadena, CA, Jet Propulsion Laboratory 93-24, 148 p.
- Ford, P.G., and Pettengill, G.H., 1992, Venus topography and kilometer-scale slopes: *Journal of Geophysical Research*, v. 97, p. 13,103-13,114.
- Ghent, R. R. and Tibuleac, I. M., 2002, Ribbon spacing in Venusian tessera: Implications for layer thickness and thermal state, *Geophysical Research Letters*, 29, No. 20, 2000, 61-1-4.
- Glaze, L. S., Stofan, E. R., Smrekar, S. E., Baloga, S. M., 2002, Insights into corona formation through statistical analyses, *Journal of Geophysical Research*, v. 107, no. E12, p. 18-1.
- Hansen, V.L., 2006, Geologic constraints on crustal plateau surface histories, Venus: The lava pond and bolide impact hypothesis: *Journal of Geophysical Research*, v. 111.
- Hansen, V.L., and Young, D.A., Accepted, Venus evolution: An alternate view: GSA Special Paper: Convergent Margin Tessera and Associated Regions.
- Hansen, V. L., Nordberg, T., and Lopez, I., 2006, Venus was not catastrophically resurfaced, in 2006 Annual Geological Society of America meeting, Abstract # 123-2, Geological Society of America, Boulder, CO.
- Hansen, V. L., Banks, B. K., and Ghent, R. R., 1999, Tessera terrain and crustal plateaus, Venus, *Geology*, v. 27, no. 12, p. 1071-1074.
- Head, J.W., and Basilevsky, A.T., 1998, Sequence of tectonic deformation in the history of Venus: Evidence from global stratigraphic relationships: *Geology*, v. 26, p. 35-38.
- Herrick, R. R. and Sharpton, V. L., 2000, Implications from stereo-derived topography of Venusian impact craters, *Journal of Geophysical Research*, v. 105, no. E8, p. 20,245-20,262.
- Herrick, R.R., Sharpton, V.L., Malin, M.C., Lyons, S.N., and Feely, K., 1997, Morphology and morphometry of impact craters, *in* Bougher, S.W., Hunten, D.M., and Phillips, R.J., eds., *Venus II: Geology, Geophysics, Atmosphere, and Solar Wind Environment*: Tucson, AZ, The University of Arizona Press, p. 1015-1046.
- Hoerz, F., Cintala, M., Rochelle, W. C., Mitchell, C. M., Smith, R. N., Dobarco-Otero, J., Finch, B. K., See, T. H., 2004, Atmospheric entry studies and the smallest impact craters on Mars, in *Lunar and Planetary Science XXXV*, Abstract # 1116, Lunar and Planetary Institute, Houston, (CD-ROM).
- Ivanov, M. A. and Head, J. W., 1996, Tessera terrain on Venus: A survey of the global distribution, characteristics, and relation to surrounding units from Magellan data, *Journal of Geophysical Research*, v. 101, no. E6, p. 14861-14908.
- Izenberg, N.R., Arvidson, R.E., and Phillips, R.J., 1994, Impact crater degradation on Venusian plains: *Geophysical Research Letters*, v. 21, p. 289-292.
- Kagan, Y.Y., and Knopoff, L., 1980, Spatial distribution of earthquakes: The two-point distribution problem: *Geophysical Journal of the Royal Astronomical Society*, v. 62, p. 303-320.
- Kearey, P. and Vine, F., 1996, *Global Tectonics*: Malden, MA, Blackwell Science Ltd., 333 p.
- Lancaster, M. G., Guest, J. E., and Magee, K. P., 1995, Great lava flow fields on Venus, *Icarus*, v. 118, no. 1, p. 69-86.

- Lellouch, E., Clancy, T., Crisp, D., Kliore, A.J., Titov, D., and Bougher, S.W., 1997, Monitoring of mesosphere structure and dynamics, *in* Bougher, S.W., Hunten, D.M., and Phillips, R.J., eds., *Venus II: Geology, Geophysics, Atmosphere, and Solar Wind Environment*: Tucson, AZ, The University of Arizona Press, p. 295-324.
- McGill, G. E., 1994, Hotspot evolution and Venusian tectonic style, *Journal of Geophysical Research*, v. 99, no. 23, p. 23149-23161.
- McKenzie, D., Ford, P.G., Johnson, C., Parsons, B., Sandwell, D., Saunders, S., and Solomon, S.C., 1992, Features on Venus generated by plate tectonic boundary processes: *Journal of Geophysical Research*, v. 97, p. 13,533-13,544.
- McKinnon, W.B., Zahnle, K.J., Ivanov, B.A., and Melosh, H.J., 1997, Cratering on Venus: Models and observations, *in* Bougher, S.W., Hunten, D.M., and Phillips, R.J., eds., *Venus II: Geology, Geophysics, Atmosphere, and Solar Wind Environment*: Tucson, AZ, The University of Arizona Press, p. 969-1014.
- Nimmo, F. and McKenzie, D., 1998, Volcanism and tectonism on Venus, *Annual Review of Earth and Planetary Sciences*, v. 26, p. 23-51.
- Paramentier, E. M., Hess, P. C., and Sotin, C., 1993, Mechanisms for episodic large-scale mantle overturn with application to catastrophic resurfacing of Venus, *Eos Transactions of the American Geophysical Union (Supplemental)*, 74(16), p. 188.
- Paramentier, E. M. and Hess, P. C., 1992, Chemical differentiation of a convecting planetary interior: Consequences for a one-plate planet such as Venus, *Geophysical Research Letters*, v. 19, p. 2015-2019.
- Phillips, R. J., 1993, The age spectrum of the Venusian surface: *Eos Transactions of the American Geophysical Union (Supplemental)*, 74(16), p. 187.
- Phillips, R.J., and Hansen, V.L., 1998, Geological evolution of Venus: Rises, plains, plumes, and plateaus: *Science*, v. 279, p. 1492-1497.
- Phillips, R.J., and Izenberg, N.R., 1995, Ejecta correlations with spatial crater density and Venus resurfacing history: *Geophysical Research Letters*, v. 22, p. 1517-1520.
- Phillips, R.J. and Hansen, V.L., 1994, Tectonic and magmatic evolution of Venus: *Annual Reviews of Earth and Planetary Sciences*, v. 22, p. 597-654.
- Phillips, R.J., Raubertas, R.F., Arvidson, R.E., Sarkar, I.C., Herrick, R.R., Izenberg, N.R., and Grimm, R.E., 1992, Impact craters and Venus resurfacing history: *Journal of Geophysical Research*, v. 97, p. 15,923-15,948.
- Phillips, R. J., Arvidson, R. E., Boyce, J. M., Campbell, D. B., Guest, J. E., Schaber, G. G., and Soderblom, L. A., 1991, Impact craters on Venus: Initial analysis from Magellan: *Science*, v. 252, p. 288-297.
- Phillips, R. J., Kaula, W. M., McGill, G. E., and Malin, M. C., 1981, Tectonics and evolution of Venus, *Science*, v. 220, p. 879-887.
- Saunders, R.S., Spear, A.J., Allin, P.C., Austin, R.S., Berman, A.L., C., C.R., Clark, J., DeCharon, A.V., De Jong, E.M., Griffith, D.G., Gunn, J.M., Hensley, S., Johnson, W.T.K., Kirby, C.E., Leung, K.S., Lyons, D.T., Micheals, G.A., Miller, J., Morris, R.B., Morrison, A.D., Pierson, R.G., Scott, J.F., Shaffer, S.J., Slonski, J.P., Stofan, E.R., Thompson, T.W., and Wall, S.D., 1992, Magellan mission summary: *Journal of Geophysical Research*, v. 97, p. 13,067-13,090.

- Schaber, G.G., Kirk, R.L., and Strom, R.G., 1998, Data Base of Impact Craters on Venus Based on Analysis of Magellan Radar Images and Altimetry Data: Flagstaff, AZ, USGS.
- Schaber, G.G., Strom, R.G., Moore, H.J., Soderblom, L.A., Kirk, R.L., Chadwick, D.J., Dawson, D.D., Gaddis, L.R., Boyce, J.M., and Russell, J., 1992, Geology and distribution of impact craters on Venus: What are they telling us?: *Journal of Geophysical Research*, v. 97, p. 13,257-13,301.
- Schultz, R. A., and Frey, H. V., 1990, A new survey of multiring impact basins on Mars, *Journal of Geophysical Research*, v. 95, no. B9, p. 14175-14189.
- Smrekar, Se. E., Kiefer, W. S., and Stofan, E. R., 1997, Large Volcanic Rises on Venus, in Bougher, S.W., Hunten, D.M., and Phillips, R.J., eds., *Venus II: Geology, Geophysics, Atmosphere, and Solar Wind Environment*: Tucson, AZ, The University of Arizona Press, p. 845-879.
- Solomon, S. C., 1993, A tectonic resurfacing model for Venus, in *Lunar and Planetary Science XXXIX*, Abstract # 2410, Lunar and Planetary Institute, Houston, p. 1331-1332.
- Steinbach, V. and Yuen, D. A., 1992, The effects of multiple phase transitions on Venusian mantle convection, *Geophysical Research Letters*, v. 19, no. 22, p. 2243-2246.
- Strom, R.G., Schaber, G.G., and Dawson, D.D., 1994, The global resurfacing of Venus: *Journal of Geophysical Research*, v. 99, p. 10,899-10,926.
- Surkov, I.A., Moskaleva, L.P., Khariukova, V.P., Dudin, A.D., and Smirnov, G.G., 1986, Venus rock composition at the Vega 2 landing site: *Journal of Geophysical Research*, v. 91, p. 215-218.
- Turcotte, D.L., Morein, G., Roberts, D., and Malamud, B.D., 1999, Catastrophic resurfacing and episodic subduction on Venus: *Icarus*, v. 139, p. 49-54.
- Turcotte, D.L., 1993, An episodic hypothesis for Venusian tectonics, *Journal of Geophysical Research*, v. 98, p. 17,061-17,068.
- Walpole, R.E., Myers, R.H., Myers, S.L., and Ye, K., 2007, *Probability and Statistics for Engineers and Scientists*: Upper Saddle River, NJ, Pearson Prentice Hall, 816 p.